Syst. Biol. 63(2):134–152, 2014
© The Author(s) 2013. Published by Oxford University Press, on behalf of the Society of Systematic Biologists. All rights reserved.
For Permissions, please email: journals.permissions@oup.com
DOI:10.1093/sysbio/syt070
Advance Access publication December 4, 2013

Introgression and Phenotypic Assimilation in *Zimmerius* Flycatchers (Tyrannidae): Population Genetic and Phylogenetic Inferences from Genome-Wide SNPs

FRANK E. RHEINDT[1,2,3,*], MATTHEW K. FUJITA[2,3,4], PETER R. WILTON[2,3], AND SCOTT V. EDWARDS[2,3]

[1]*Department of Biological Sciences, National University of Singapore, 14 Science Drive 4, Singapore 117543;* [2]*Department of Organismic and Evolutionary Biology, Harvard University, 26 Oxford Street, Cambridge, MA 02138, USA;* [3]*Museum of Comparative Zoology, 26 Oxford Street, Cambridge, MA 02138, USA; and* [4]*Department of Biology, University of Texas at Arlington, Arlington, TX 76019, USA*
**Correspondence to be sent to: Department of Biological Sciences, National University of Singapore, 14 Science Drive 4, Singapore 117543; E-mail: dbsrfe@nus.edu.sg.*

Received 14 May 2013; reviews returned 17 July 2013; accepted 18 November 2013
Associate Editor: John McCormack

Abstract.—Genetic introgression is pervasive in nature and may lead to large-scale phenotypic assimilation and/or admixture of populations, but there is limited knowledge on whether large phenotypic changes are typically accompanied by high levels of introgression throughout the genome. Using bioacoustic, biometric, and spectrophotometric data from a flycatcher (Tyrannidae) system in the Neotropical genus *Zimmerius*, we document a mosaic pattern of phenotypic admixture in which a population of *Zimmerius viridiflavus* in northern Peru (henceforth "mosaic") is vocally and biometrically similar to conspecifics to the south but shares plumage characteristics with a different species (*Zimmerius chrysops*) to the north. To clarify the origins of the mosaic population, we used the RAD-seq approach to generate a data set of 37,361 genome-wide single nucleotide polymorphisms (SNPs). A range of population-genetic diagnostics shows that the genome of the mosaic population is largely indistinguishable from southern *Z. viridiflavus* and distinct from northern *Z. chrysops*, and the application of parsimony and species tree methods to the genome-wide SNP data set confirms the close affinity of the mosaic population with southern *Z. viridiflavus*. Even so, using a subset of 2710 SNPs found across all sampled lineages in configurations appropriate for a recently proposed statistical ("ABBA/BABA") test that distinguishes gene flow from incomplete lineage sorting, we detected low levels of gene flow from northern *Z. chrysops* into the mosaic population. Mapping the candidate loci for introgression from *Z. chrysops* into the mosaic population to the zebra finch genome reveals close linkage with genes significantly enriched in functions involving cell projection and plasma membranes. Introgression of key alleles may have led to phenotypic assimilation in the plumage of mosaic birds, suggesting that selection may have been a key factor facilitating introgression. [gene flow; hybridization; *Zimmerius*; tyrant-flycatcher.]

Hybridization has been known since early historic times (Stamos 2003). Darwin (1859) employed the existence of hybrids as a vital argument against the constancy of species. Mayr (1963) recognized hybrids as an important albeit occasional product between species whose isolating mechanisms are incomplete. Because of hybrids' frequent non-viability, Mayr (1963) and many biologists of his day argued that hybridization contributes little gene flow and has no considerable impact on a species' trajectory. However, in recent decades, evidence for genetic introgression and gene flow between species has been accumulating: introgression is known to be pervasive over a wide range of organisms (e.g., see reviews by Mallet 2005; Nolte and Tautz 2010; Rheindt and Edwards 2011; Feder et al. 2012). Indeed, even humans are thought to possess up to 6% introgressed DNA from closely related recently extinct hominin lineages (Green et al. 2010; Reich et al. 2010).

Although sometimes thought to be more prevalent among neutral loci (Currat et al. 2008), introgression has been demonstrated for loci under selection (Nolte et al. 2009), or suggested to be driven by positive selection (Gompert et al. 2012; Staubach et al. 2012). Assuming that introgression in loci under selection is more often accompanied by phenotypic effects than in neutral loci, introgression may therefore have an impact on the evolutionary trajectory of recipient populations. For instance, during the colonization of new habitats by introgressive swarms of closely related species such as Darwin's finches or cichlid fish, introgression may be the agent that introduces genetic novelty into recipient species, resulting in phenotypic or behavioral adaptations (Seehausen 2004; Grant and Grant 2010).

There is still a scarcity of data on whether phenotypic changes in admixed populations are always accompanied by high levels of genomic introgression. Introgression of few key alleles or chromosomal regions may lead to substantial phenotypic assimilation of an admixed population while the majority of its genome retains ancestral variants (Anderson et al. 2009). This scenario may be more common than previously thought, since recent work has shown that single mutations in key loci can lead to great phenotypic changes across many vertebrates (Doucet et al. 2004; Mundy et al. 2004; Uy et al. 2009; Cibois et al. 2012).

In this study, we investigate genomic patterns of ancestry and introgression in a tyrant-flycatcher (Tyrannidae, Aves) complex that bears hallmarks of phenotypic admixture. The *Zimmerius viridiflavus* complex is known from mid-elevation woodlands and forest edge (500–2600 m) along Andean slopes in South America (Traylor 1979; Ridgely and Tudor 1994; Ridgely and Greenfield 2001; Fitzpatrick 2004; Schulenberg et al. 2007; Fig. 1). The complex seems to be monophyletic (Rheindt et al. 2008a) and is divided into a northern species with grayish-white underparts and a deflected call (*Zimmerius chrysops*) and a southern species with

Downloaded from http://sysbio.oxfordjournals.org/ at Ernst Mayr Library of the Museum Comp Zoology, Harvard University on February 24, 2014

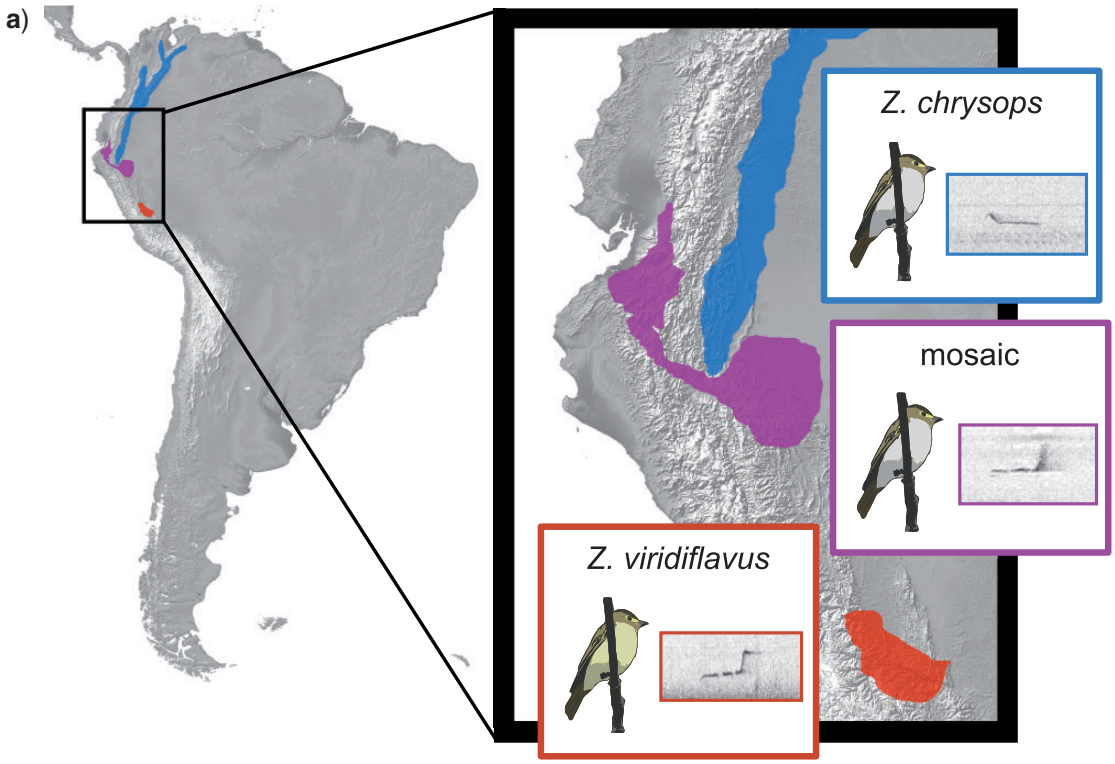

b)

Z. viridiflavus (southern)	mosaic population	*Z. chrysops* (northern)
yellow belly	gray belly	gray belly
inflected call	inflected call	deflected call
mitochondrial haplotype **A**	mitochondrial haplotype **A**	mitochondrial haplotype **B**

FIGURE 1. a) Distribution of the *Z. viridiflavus* complex in cloud forest and woodlands between 500 and 2600 m in South America (large map) and in northern Peru and Ecuador (insert). Sonograms of primary vocalizations are given for each taxon group. Blue: *Z. chrysops* (white-bellied; deflected call note); red: *Z. viridiflavus* (yellow-bellied; inflected call note); purple: mosaic populations with a *chrysops* plumage type but a *viridiflavus* call type (white-bellied, inflected call note). The black line through the mosaic (purple) range divides an unnamed population from the Peruvian departments of SMsA (east/right of the line) from the subspecies *flavidifrons* (west/left of the line). It is unclear whether there is a current geographic connection between SMsA and *flavidifrons* across the Porculla Pass (2140 m), but this connection is likely to have been in existence in the recent past. Sonograms from Rheindt et al. (2008a). b) Tabular listing of major characters reported to differ among *Z. viridiflavus*, *Z. chrysops*, and mosaic birds before this study.

yellow underparts and an inflected call (*Z. viridiflavus*; Fig. 1; Zimmer 1941; Traylor 1979; Ridgely and Tudor 1994; Ridgely and Greenfield 2001; Fitzpatrick 2004; Schulenberg et al. 2007). Recently, some geographically intermediate populations (purple in Fig. 1) were discovered to exhibit a mosaic of traits of *Z. chrysops* and *Z. viridiflavus* (Schulenberg et al. 2007; Rheindt et al. 2008a). These intermediate or phenotypically mosaic (henceforth "mosaic") populations include an unnamed population in the Peruvian departments of San Martín and southern Amazonas (henceforth SMsA) and the subspecies *flavidifrons* from the opposite western

Downloaded from http://sysbio.oxfordjournals.org/ at Ernst Mayr Library of the Museum Comp Zoology, Harvard University on February 24, 2014

slope of the Andes (Fig. 1). Mosaic populations utter calls that are virtually identical (SMsA) or similar (*flavidifrons*) to *Z. viridiflavus* even though their plumage is either identical (SMsA) or very similar (*flavidifrons*) to *Z. chrysops* (Zimmer 1941; Traylor 1979; Schulenberg et al. 2007; Rheindt et al. 2008a; Fig. 1). Mosaic birds were recently shown to share a near-identical mitochondrial (mtDNA) haplotype with *Z. viridiflavus* (Rheindt et al. 2008a; Fig. 1). In its northern geographic distribution, the mosaic population approaches the range of *Z. chrysops* to within a few kilometers along the narrow Marañón river valley: the latter is not regularly inhabited by either form because it is below the preferred elevation of this complex and possibly too dry. To the south, on the other hand, mosaic birds are separated from *Z. viridiflavus* by a distributional gap of 200–300 km of apparently suitable cloud forest that may have been inhabited by these birds in the recent past (Fig. 1).

Carotenoids, which are mainly consumed through fruit and other plant food, are the pigments generally underlying yellow plumage coloration in birds (McGraw 2004), probably including that of the yellow underparts of *Z. chrysops* and mosaic birds. However, geographic differences in diet are unlikely to have caused the yellow versus grayish-white differences in underparts coloration in the *Z. viridiflavus* complex because fruit is only a secondary source of food in the insectivorous genus *Zimmerius* (Fitzpatrick 2004). Additionally, differential intake of carotenoids usually leads to a continuum of different intensities and extents of red, orange and/or yellow in plumage, often within single populations (McGraw and Hill 2000; McGraw 2004), in contrast to the bimodal pattern of yellow versus white seen in various populations of the *Z. viridiflavus* complex. Therefore, it has been suggested that the mosaic phenotypic pattern may be due to genetic introgression (Rheindt et al. 2008a), a phenomenon that is thought to be found in various members of the tyrant-flycatcher family (e.g., Rheindt et al. 2009a).

Five scenarios may explain this pattern of potential phenotypic admixture (Fig. 2). (1) The call and mtDNA of mosaic birds may indicate their true genomic affinity with southern *Z. viridiflavus* while plumage characters may have recently introgressed from *Z. chrysops* from

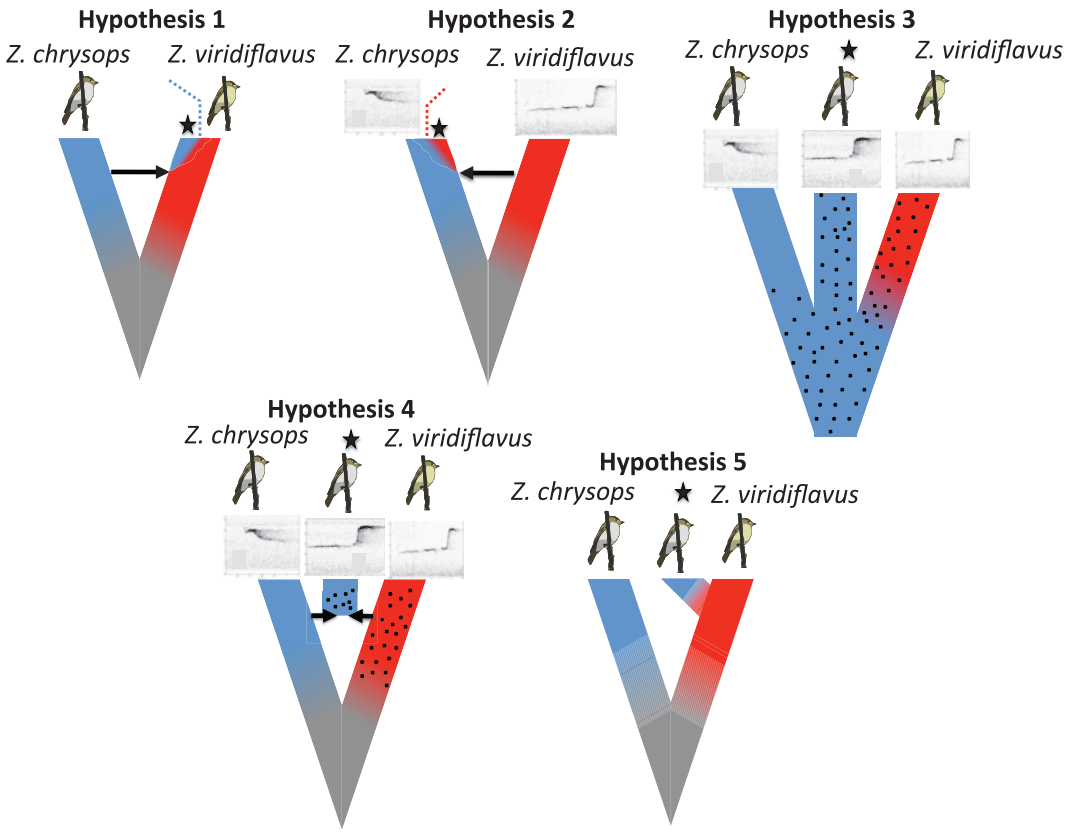

FIGURE 2. Five hypotheses for the origin of mosaic populations, which are indicated with a black asterisk. Hypothesis 1: mosaic populations may be conspecific with *Z. viridiflavus* but have experienced introgressive admixture of plumage traits (indicated in blue) from *Z. chrysops* (wholesale plumage assimilation). Hypothesis 2: mosaic populations may be conspecific with *Z. chrysops* but have experienced introgressive admixture of vocal traits and mtDNA (indicated in red) from *Z. viridiflavus*. Hypothesis 3: mosaic populations may form a deeply diverged species-level lineage that has retained ancestral vocal traits (stippled) and plumage traits (in blue), whereas *Z. chrysops* and *Z. viridiflavus* have evolved new vocal or plumage traits, respectively. Hypothesis 4: mosaic populations may be a genomic hybrid of *Z. chrysops* and *Z. viridiflavus* that ended up with plumage traits from the one (indicated by blue) and vocal traits from the other species (indicated by stippling). Hypothesis 5: mosaic populations may be a recently diverged lineage within *Z. viridiflavus* that has convergently (and independently of *Z. chrysops*) acquired a *chrysops*-like plumage pattern (indicated in blue), possibly through relatively few novel mutations.

Downloaded from http://sysbio.oxfordjournals.org/ at Ernst Mayr Library of the Museum Comp Zoology, Harvard University on February 24, 2014

the north (Rheindt et al. 2008a). The possibility of vocal evolution in *Zimmerius* is reasonable, since, as in most other suboscine passerine birds, vocalizations are likely inherited and do not change via cultural evolution (Kroodsma and Konishi 1991; Isler et al. 1998). (2) Alternatively, the *viridiflavus* mtDNA haplotype and call may have recently invaded the presumably admixed population via occasional hybridization from the south, while their actual genetic origin may lie with the equal-plumaged northern *Z. chrysops*. (3) As a third possibility, the mosaic populations may be an independent lineage whose divergence from northern *Z. chrysops* is as great as it is from southern *Z. viridiflavus*; mosaic birds may have retained the ancestral plumage and vocal phenotype while *Z. chrysops* and *Z. viridiflavus* have evolved new vocal or plumage phenotypes, respectively. (4) Mosaic birds may form a hybrid population, constituting a roughly even genomic mix of southern *Z. viridiflavus* and northern *Z. chrysops* that happened to have inherited plumage characters from the one species and vocal and mitochondrial characters from the other. (5) Finally, with recent suggestions that few mutations can sometimes bring about major phenotypic changes in traits such as bird plumage (Doucet et al. 2004; Mundy et al. 2004; Uy et al. 2009; Cibois et al. 2012), mosaic birds may form a population of southern *Z. viridiflavus* that has recently evolved yellow underparts convergently; although appearing identical to the yellow underparts of *Z. chrysops* populations from across the Marañón River, their origin would thus be independent (Fig. 2).

Here we characterize the level of morphological and vocal admixture in the *Z. viridiflavus* complex using bioacoustic, biometric, and spectrophotometric data collected from throughout its range. The spectrophotometric data are analysed using a tetracolor space model that allows us to assess color differences as seen by the birds. We then use single nucleotide polymorphism (SNP) data generated with a next-generation sequencing platform and a restriction-enzyme associated DNA (RAD) protocol to determine the genomic affinity of 12 individual flycatchers in order to verify whether the phenotypic mosaic is derived from genetic admixture via introgression or based on ancestral trait retention. We are particularly interested in determining the presence and degree of introgression to understand if limited introgression can lead to wholesale plumage assimilation.

Our study also has implications for sampling and experimental design in next-generation phylogeography and phylogenetics. Recent studies, especially in modern humans and their hominin relatives, have validated the use of small numbers of individuals, even single diploid individuals, in reconstructing broad parameters of population histories when large numbers of SNPs or whole-genome data are collected (Green et al. 2010; Gronau et al. 2011; Li and Durban 2011). For some population statistics such as genetic diversity within populations, it is well known that an increase in numbers of individuals is often accompanied by only modest increases in the precision of estimates, and that sampling more loci is favored over sampling more individuals in some situations (Felsenstein 2006; Carling and Brumfield 2007). Recent studies, particularly in humans and Neanderthals, have confirmed that sampling just a few individuals of focal species is sufficient to detect the presence of introgression, provided that sufficiently large numbers of loci are sampled (Green et al. 2010). Thus our study also contributes to the discussion of optimal sampling of natural populations for population-genetic inference in the genomic era, particularly for non-model lineages.

Materials and Methods

Phenotypic Analysis

Bioacoustic measurements.—We carried out vocal analysis of 35 call recordings that were available for this species complex from the sound library Xeno-Canto (www.xeno-canto.org) at the time of analysis (Supplementary Table S1, available at http://datadryad.org, doi:10.5061/dryad.633b; last accessed December 7, 2013). Xeno-Canto recordings are uploaded with detailed locality information as captured in satellite maps. We double-checked all call types against recording locality and confirmed that no misallocation to taxon had occurred. *Zimmerius* flycatchers are known to have two main types of vocalizations (dawn songs and call notes; Ridgely and Tudor 1994; Schulenberg et al. 2007), and we made sure to compare only homologous vocalizations. We omitted sound recordings of the rarely heard dawn song of these species because of the paucity of recordings. Our vocal database included 24 call samples of *Z. chrysops*, 4 samples of *Z. viridiflavus*, and 7 recordings of mosaic populations. The vocal sample size of *Z. viridiflavus* and mosaic populations reflects the fact that there is less ornithological fieldwork carried out in their restricted ranges compared with *Z. chrysops*. Using standard settings in RAVEN 1.4 software (Bioacoustics Research Program 2011), we scored all call recordings using seven vocal parameters: (1) minimum frequency, (2) maximum frequency, (3) frequency range, (4) dominant frequency (defined as the frequency at which there is the greatest concentration of amplitude at any single point in time), (5) frequency modulation (defined as the differential in frequency from the start to the end of the call), (6) number of call elements within each call, and (7) duration of call. Frequency modulation in the calls of the *Z. viridiflavus* complex was always unidirectional and never involved a mixture of decreasing and increasing frequencies. Hence, parameter 5 was defined as a simple frequency differential from the start to the end of the call without considering directional changes within the call.

Biometric measurements.—We also conducted biometric measurements on museum specimens from the complex. To enhance consistency, a single person (F.E.R.) measured 4 biometric parameters (length of

Downloaded from http://sysbio.oxfordjournals.org/ at Ernst Mayr Library of the Museum Comp Zoology, Harvard University on February 24, 2014

tarsus, upper mandible [henceforth: bill], wing, and total body length) for a data set containing 91 specimens from the American Museum of Natural History (New York; AMNH) and the Museum of Comparative Zoology (Cambridge, Massachusetts; MCZ; Supplementary Table S2, available at http://datadryad.org, doi:10.5061/dryad.633bk). Mann–Whitney *U* tests were used to test for differences in biometric data between sexes and among populations.

Spectrophotometric measurements.—A single person (F.E.R.) made spectrophotometric measurements of crown, back, breast, and belly color of the 91 specimens that had been measured biometrically. We used a USB 2000 spectrophotometer (Ocean Optics, Dunedin, FL) with the following settings: average reading 5, integrating time 100 ms, and no boxcar smoothing. We recorded reflectance data (percent light reflected at each wavelength from 320 to 700 nm) with the reflectance probe held against the body part at an angle of 90°. We recalibrated the spectrophotometer against a barium sulphate white standard for each specimen. Three measurements were taken per body part and averaged. We analysed measurements of 63 AMNH and 28 MCZ specimens separately because they had been taken under separate lighting conditions at different locations. Because spectrophotometric taxon differences showed identical patterns between the AMNH and MCZ data sets, we only considered the larger data set (AMNH) for downstream spectrophotometric analysis (Supplementary Table S3, available at http://datadryad.org, doi:10.5061/dryad.633bk).

We computed the quantum catches, Q_i, of each single-cone cell receptor type in the avian retina: Q_u (UV-wavelength sensitive), Q_s (short-wavelength sensitive), Q_m (medium-wavelength sensitive), Q_l (long-wavelength sensitive), and their corresponding noise-to-signal ratios. There is minimal variation across perching birds in the wavelengths of peak sensitivity for all four single-cone cell types (Hart and Hunt 2007). Following Eaton (2005), we used spectral sensitivity function data for the blue tit *Cyanistes caeruleus* as a representative passerine visual system. With spectral sensitivity data or cone cell type proportions being unavailable for *Zimmerius* flycatchers, we derived noise-to-signal ratios from the proportions of each of the single-cone cell types found in the blue tit retina. Eaton (2005) and Benites et al. (2010) compared color space distances using cone cell type proportions of a variety of species encompassing the known variation among passerines and failed to find significant effects on color space values. Therefore, use of the blue tit visual system for computing color space distances is justified. As a basis for plumage comparisons among taxa and populations, we used the tetracolor space model appropriate for birds (e.g., Stoddard and Prum 2008) and computed ΔS values (Vorobyev and Osorio 1998; Vorobyev et al. 1998) with the "tetradistance" script (Rafael Maia, unpublished data; Supplementary File 1 in Dryad Digital Repository, available at http://datadryad.org, doi:10.5061/dryad.633bk) implemented in R (s). These values measure how different two colors are as perceived by the birds (rather than by humans). Color differences of $\Delta S < 1$ are generally interpreted as being imperceptible to the subject's eyes under any circumstances (Osorio et al. 2004). However, in natural settings and light conditions, values of up to $\Delta S = 4$ have been considered as detectability thresholds for color differences (Osorio et al. 2004).

Statistical analysis.—We carried out principal component analysis (PCA) on the correlation matrix of vocal characters, biometric characters, and plumage reflectance values using the "prcomp" command in R (R Development Core Team 2008).

Molecular Analysis

RAD-seq protocol.—We sampled 2 *Z. viridiflavus*, 3 *Z. chrysops*, 5 birds from mosaic populations, and 2 outgroup individuals (*Z. acer, Z. gracilipes*) for molecular analysis (Supplementary Table S4, available at http://datadryad.org, doi:10.5061/dryad.633bk), for a total of 12 individuals or 24 copies for each locus. We extracted DNA using procedures employed by Rheindt et al. (2008b). The tissues we used had been preserved in ethanol for an average of ∼20 years, and we found that the quantity of DNA was insufficient for application of the RAD-seq approach, prompting us to conduct whole-genome amplification (WGA) using the REPLI-g Ultra Fast kit (Qiagen, Venlo, Netherlands) following the manufacturer's protocols to increase starting material. In previous research on human DNA (Barker et al. 2004; Han et al. 2012), WGA (using the same kits we used) produced accurate wgaDNA for subsequent application in genotyping, confirming the suitability of our approach. We used a modified version of Bers et al.'s (2010) RAD-seq protocol to construct reduced-representation libraries of genomic DNA of each individual. Briefly, we used the Illumina Hi-Seq 2000 platform to sequence genomic DNA that has been digested with a restriction enzyme. Among many individuals, these restriction fragments are largely homologous, making it a desirable approach for generating reduced-representation genomic surveys among several individuals. However, because individuals not possessing recognition sites in one or both chromosomes will not be targeted by a given enzyme, the RAD-seq method can yield downwardly biased estimates of population variability (Arnold et al. 2013). For DNA digestion, we used the restriction enzyme *Sbf*1 (New England Biolabs, Ipswich, Massachusetts), which has an 8 bp recognition site (5′-CCTGCAGG-3′). We purified the digest using a Qiagen DNEasy column (Qiagen, Venlo, Netherlands) according to manufacturers' specifications. We then size-selected our fragmented genomic DNA for 400–1000 bp fragments by excising the appropriate fragments from a 1% agarose gel and purifying using a Qiaquick gel extraction kit

Downloaded from http://sysbio.oxfordjournals.org/ at Ernst Mayr Library of the Museum Comp Zoology, Harvard University on February 24, 2014

(Qiagen, Venlo, Netherlands). Subsequently, we used Fragmentase (New England Biolabs, Ipswich, Massachusetts) according to the manufacturer's protocols to shear DNA molecules to ~300–600 bp fragments. After shearing, we used the NEBNext Sample Preparation Kit (New England Biolabs, Ipswich, Massachusetts) to end-repair sequences and add A-tails. Finally, we ligated Illumina flowcell-compatible barcoded adapters (Bio-O Scientific; www.biooscientific; barcodes listed in Supplementary Table S4, available at http://datadryad.org, doi:10.5061/dryad.633bk). We carried out a second round of size selection, this time for 400–500 bp fragments following the previous procedure, to remove unligated or erroneously ligated adapters. We carried out a final PCR using Phusion polymerase (New England Biolabs, Ipswich, Massachusetts) according to the manufacturer's protocols to enrich DNA and conducted another round of purification using a Qiaquick PCR purification kit (Qiagen, Venlo, Netherlands) according to the manufacturer's instructions. We used Qubit Fluorometric Quantitation (Invitrogen, Carlsbad, California), an Agilent 2100 Bioanalyzer (Agilent, Santa Clara, California), and qPCR to ensure an appropriate amount and fragment size distribution of template for 100 bp paired-end sequencing on a single Illumina flowcell at the Bauer Core Laboratory at Harvard University using CASAVA v 1.7.0 software with the error correction for index sequences turned off. Prior to Illumina sequencing, we cloned a small proportion of the volume of mixed libraries and sequenced several clones to confirm successful adapter ligation in the correct orientation and presence of barcodes and expected *Sbf*1 recognition sites.

Computational analysis and bioinformatics.—We used the fastx suite of tools to process the original reads (http://hannonlab.cshl.edu/fastx_toolkit): we first removed contaminating adapters using fastx_clipper; we then trimmed the ends of the sequences for bases with quality scores <20 using fastq_quality_trimmer; finally, we removed any reads that had more than 10% bases whose quality scores were 20 or less. To align sequences against one another in the absence of a reference genome, we created a pseudo-reference genome (PRG) using Velvet (Zerbino and Birney 2008) with the maximum "kmer" value 31 and a coverage cut-off of 5. As linkage information was required for some of the analyses, we leveraged the putatively conserved chromosomal synteny in birds (Ellegren 2010) by mapping the contigs of our PRG to the zebra finch (*Taeniopygia guttata*) genome (Ensembl assembly number 3.2.4) using BLASTN (see Supplementary File 2, available at http://datadryad.org, doi:10.5061/dryad.633bk for FASTA sequence labels of the zebra finch chromosome sequences used). We considered a contig successfully mapped if it had only one hit against the zebra finch genome and that hit had an e-value $<10^{-20}$ (see Supplementary File 3, available at http://datadryad.org, doi:10.5061/dryad.633bk for tabular BLASTN results).

We then aligned reads against the PRG using "bwa 0.6.1-r104" (Li and Durbin 2009) and samtools (http://samtools.sourceforge.net) for subsequent SNP calling. We identified SNPs in our mapped reads using VarScan 2.2.8 (Koboldt et al. 2012) by running the "mpileup2snp" command with the parameter settings "–min-coverage 20" and "–*P*-value 0.05" (Supplementary File 4, available at http://datadryad.org, doi:10.5061/dryad.633bk). No adjustments or quality score recalibrations for SNP calls around indels were made. After visually assessing allele distribution among reads across individuals and loci, we concluded that the following genotyping scheme most realistically classifies polymorphisms into SNP classes: SNPs with a coverage of ≥20X in which 0–10% of reads were identical to the PRG are considered homozygote variants, those in which 20–80% were identical to the PRG are considered heterozygotes and those in which 90–100% are identical are considered homozygote non-variants. We discarded SNPs in which 10–20% or 80–90% were identical because it is not clear whether those could be hetero- or homozygotes. We chose not to use the Fisher's exact test *P*-values provided by VarScan 2.2.8 in our genotyping scheme because the *P*-values indicate only the probability that a given individual is a non-variant. Thus they are sensitive to choice of consensus and variant bases. Our cut-offs provide some assurance that the heterozygous calls are supported by a ratio of reads in agreement with a heterozygous genotype; in concept this is similar to the methods developed in Martin et al. (2010).

Population structure.—We utilized the program STRUCTURE (Pritchard et al. (2000)) to evaluate the genomic affinity of individuals. We carried out three replications of a STRUCTURE run with two clusters ($K = 2$) to test whether mosaic birds cluster with *Z. chrysops*, *Z. viridiflavus*, or a combination thereof. In addition, we did the same for three clusters ($K = 3$) to test whether individuals from the mosaic population consistently form a lineage of their own, or whether they are genetically indistinguishable from either *Z. chrysops* or *Z. viridiflavus*. We ran STRUCTURE with all SNPs polymorphic in the ingroup lineages ($n = 33{,}069$), but we conducted additional STRUCTURE runs (1) with a subset of SNPs that have at least one SNP call in each of the four lineages, counting the two outgroups as one lineage ($n = 8788$); (2) with a subset of SNPs that mapped to the zebra finch genome ($n = 9525$); (3) with a subset of only one SNP per contig ($n = 11{,}475$).

To complement our analysis with STRUCTURE, we also carried out PCA using the software SMARTPCA (Patterson et al. (2006)). Missing data can bias PCA results if the pattern of missing data shows population structure (Patterson et al. 2006). Missing data in our data set may have shown some population structure (Supplementary Fig. S1, available at http://datadryad.org, doi:10.5061/dryad.633bk), so we included only sites at which all ingroup individuals were called ($n = 1288$) in all PCA analyses.

Downloaded from http://sysbio.oxfordjournals.org/ at Ernst Mayr Library of the Museum Comp Zoology, Harvard University on February 24, 2014

As another way to evaluate differentiation between the three focal populations, we calculated F_{ST}-values among populations and/or taxa using a recent estimator specifically devised to take into account small or uneven sample sizes (Reich et al. 2009) and shown to perform well with such data sets (Willing et al. 2012). We also performed a permutation test that is based on the calculation of K_{ST}-values among populations followed by a permutation of individual population labels (Hudson et al. 1992a). All F_{ST} and K_{ST} calculations were performed using a custom-written script (Supplementary File 5, available at http://datadryad.org, doi:10.5061/dryad.633bk). F_{ST} and K_{ST} are complementary measures of population differentiation, with F_{ST} being based solely on allele frequencies (Hudson et al. 1992b) and K_{ST} based on the mean number of differences between sequences sampled within and across all populations (Hudson et al. 1992a). The number of individuals sampled was too few to permute population labels once for each permutation replicate. Instead, for each permutation replicate we permuted population labels independently for each locus to construct a set of shuffled "genomes" against which the actual data could be compared. Using the software MS (Hudson 2002), we simulated appropriately sized sets of SNPs in linkage equilibrium in a two-subpopulation model across a range of migration rates and found no difference in power or error between this approach and the test as originally devised by Hudson (2002, results not shown). Because the K_{ST} statistic requires a fixed sample size for the two populations being considered, we used only SNPs called in all individuals of both populations for each pairwise test. Additionally, because the above modifications to the test require linkage equilibrium between loci, we randomly sampled one such SNP from each contig for inclusion in the test (*viridiflavus-chrysops*, $n = 1311$; *viridiflavus*-mosaic, $n = 611$; *chrysops*-mosaic, $n = 584$). To further assess sensitivity, we performed the same test of differentiation on SNPs taken from individuals from the same population.

Phylogenetic analysis.—We used the Bayesian software SNAPP (Bryant et al. 2012) to estimate a species tree from the data set that included all SNPs represented in all individuals, including outgroups ($n = 954$), regardless of whether they mapped to the zebra finch genome or not. In addition, we carried out SNAPP analyses on a subset ($n = 947$) in which we removed all sites found to be heterozygous across all individuals. We did this to avoid including a class of SNPs with an unexpected genotype distribution across species; these SNPs may be under balancing selection or possibly mis-genotyped. We found no qualitative difference in topology and branch lengths between the two types of analysis, and we therefore only report those results based on the 954-SNP data set. SNAPP estimates species trees from unlinked SNPs, a data type that cannot yield gene trees as intermediates between DNA sequences and species trees (Edwards 2009; Bryant et al. 2012). SNAPP yields a species tree topology with branch lengths in units of substitutions per site as well as population sizes in units of $N = \theta/4\mu$ individuals (with μ being the expected number of mutations per site per generation and θ being average divergence between two individuals). We used default settings for most parameters, and analyses were checked for convergence using TRACER (Rambaut and Drummond 2007), making sure that Bayesian runs reached an effective sample size >200 after burn-in. We selected a gamma distribution to account for the θ prior using a set of alpha and beta parameters allowing for different current and ancestral population sizes: (1) a gamma (2,2000) prior (with $\bar{\theta} = 0.001$) for small population sizes, and (2) a gamma (1,10) prior (with $\bar{\theta} = 0.1$) for large population sizes. Analysis with the two priors produced the same topology, so we only report the estimates using large population sizes. We additionally carried out SNAPP analyses on SNP subsets in which either the mosaic population or the southern species (*Z. viridiflavus*) was removed to investigate effects of gene flow and taxon sampling on the results. We visualized the posterior distribution of species trees using the software DensiTree (Bouckaert 2010).

To explore phylogenetic relationships, we constructed parsimony trees using a stepmatrix in which each genotype is one step from the adjacent one sharing one allele, with heterozygotes being one step from each homozygote but the two homozygotes being two steps from each other. We generated these trees using PAUP v. 4.0a126 (Swofford 2003; see Supplementary File 6, available at http://datadryad.org, doi:10.5061/dryad.633bk for the NEXUS file used in this analysis).

Test of introgression and gene ontology enrichment.—Genetic introgression has traditionally been detected by using sequence-based modeling of marker-specific coalescent times (e.g., Garrigan and Hammer 2006; Fuchs et al. 2013) or by the fortuitous detection of rare genomic changes (e.g., McCormack and Venkatraman 2013). However, the recently developed "ABBA/BABA" test (Green et al. 2010; Durand et al. 2011; see also Kulathinal et al. 2009) allows for the detection of genetic introgression in next-generation sequencing data. Using custom-written scripts (Supplementary File 5, available at http://datadryad.org, doi:10.5061/dryad.633bk), we evaluated the test using *D*-statistics, originally developed to test for admixture between Neanderthals and modern humans (Green et al. 2010; Durand et al. 2011; Fig. 3). We first calculated the sample frequency of the PRG variant allele in each population and used equation (2) in Durand et al. (2011) to calculate *D*. For these tests, we considered only sites meeting two criteria. (1) Sites were required to be called in at least one individual of *Z. viridiflavus*, mosaic birds, *Z. chrysops*, and at least one outgroup. This criterion simply reflects the phylogenetic distribution of alleles among ingroups and outgroups required to conduct the test (Green et al. 2010; Durand et al. 2011; Fig. 3), which measures the departure from equality of SNPs

Downloaded from http://sysbio.oxfordjournals.org/ at Ernst Mayr Library of the Museum Comp Zoology, Harvard University on February 24, 2014

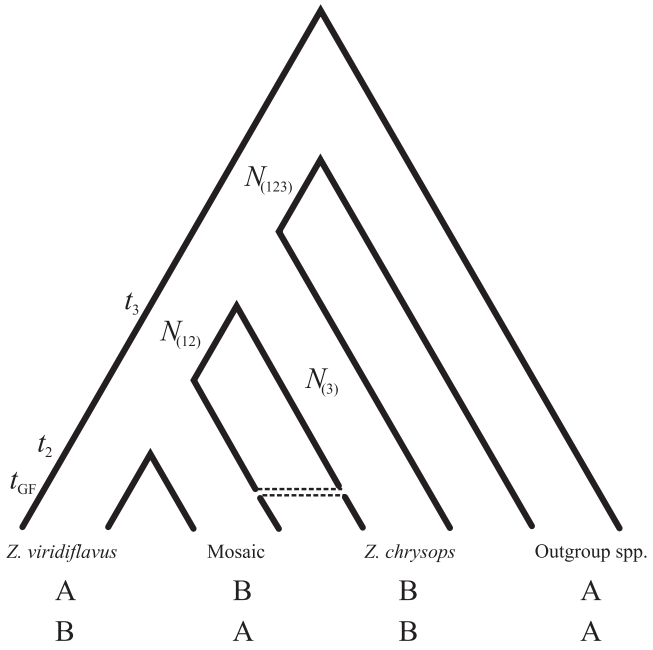

FIGURE 3. A scenario for introgression between *Z. chrysops* and the mosaic population, with a single episode of widespread gene flow. Population-genetic parameters (divergence time-points *t* and ancestral population sizes *N*) are given. The ABBA–BABA pattern of SNP call distribution includes only those SNPs in which the outgroup differs from the presumable introgression donor species (*Z. chrysops*) and in which the presumably admixed population (mosaic) also differs from its presumable parent population (*Z. viridiflavus*). Although both patterns (ABBA and BABA) are consistent with incomplete lineage sorting, only ABBA is consistent with introgression from *Z. chrysops* into mosaic populations. Therefore, one would expect an equal incidence of ABBA and BABA under incomplete lineage sorting but a higher incidence of ABBA if introgression has occurred.

that exhibit a pattern of shared polymorphism that could be due either to incomplete lineage sorting or gene flow. (2) Sites were required to be on a contig that had been mapped to the zebra finch genome. We separately recorded the percentage of ABBA–BABA sites that mapped against the zebra finch Z chromosome. The ABBA–BABA test requires a sample large enough to assume that the distribution of *D* is approximately normal and that there is linkage equilibrium among sampled chromosomal regions. We estimated the standard error of *D* by jackknifing over linkage blocks using the zebra finch chromosomal positions (see, e.g., Green et al. 2010). Because we do not know the extent of linkage disequilibrium in the *Zimmerius* genome, we performed this jackknife estimate of the standard error multiple times over a large range of linkage block sizes.

Following Green et al. (2010) and Durand et al. (2011), we also calculated a fraction of admixture between *Z. chrysops* and the mosaic population using our observed value of *D*. This fraction is the fraction of ancestral mosaic lineages following the admixture path in the model of instantaneous admixture (Fig. 3). In order to make these calculations accurately, it is necessary to have some knowledge of the ancestral population sizes (*N*) and divergence dates (*t*) in this model (Fig. 3). These parameters are largely unknown in *Zimmerius*, and because we found that the posteriors of *N* and *t* depend strongly on the priors used, we allowed all of the relevant parameters to vary freely over a reasonable set of values (Supplementary Table S5, available at http://datadryad.org, doi:10.5061/dryad.633bk). We then maximized the expression for the admixture fraction—from solving equation [S19.5] in Green et al. (2010)—over the resulting parameter space in order to produce a maximum value for the admixture. We also calculated a separate upper bound for the admixture fraction using equation [8] in Durand et al. (2011). This second calculation requires no knowledge of ancestral population sizes and divergence dates. In order to calculate this latter quantity it was necessary to split our *Z. chrysops* sample into two different groups (cf. $P_{3,1}$, $P_{3,2}$ in equation [8] of Durand et al. 2011). We performed the calculation for all possible splittings of the *Z. chrysops* sample and averaged all values to produce an estimate of the upper bound. For all calculations related to the admixture fraction, we included all SNPs for which at least one genotype was available for all lineages involved.

For those ABBA/BABA sites that mapped onto the zebra finch genome, we searched for the nearest gene on the chromosome and recorded its distance from the ABBA/BABA site. To explore the potential linkage of ABBA or BABA sites with genes under selection, we categorized SNPs as "ABBA-like" and "BABA-like" based on the allele frequencies at the site (with ABBA-like SNPs having allele frequencies more reflective of the ABBA pattern than the BABA pattern, and *vice versa*). We then used a custom-made script (Supplementary File 7, available at http://datadryad.org, doi:10.5061/dryad.633bk) employing the TOpGO method in Bioconductor (www.bioconductor.org) to test the distribution of gene ontology (GO) terms of genes linked to ABBA-like SNPs and genes linked to BABA-like SNPs against the distribution of GO terms in the zebra finch genome as a whole. In particular, this method searches through three types of GO terms: biological processes, cellular components, and molecular functions. We looked for an enrichment of any one of those three terms in either the ABBA or BABA-linked gene sets using Fisher's exact test and a correction for multiple testing using False Discovery Rate (FDR) as implemented in R. After these steps, we considered adjusted *P*-values <0.05 significantly enriched GO categories.

RESULTS

Phenotypic traits

Vocal measurements (Supplementary Table S1, available at http://datadryad.org, doi:10.5061/dryad.633bk), when subjected to PCA, resulted in first and second principal components that carried the overwhelming proportion (94.8%) of total variance (Supplementary Table S6, available

Downloaded from http://sysbio.oxfordjournals.org/ at Ernst Mayr Library of the Museum Comp Zoology, Harvard University on February 24, 2014

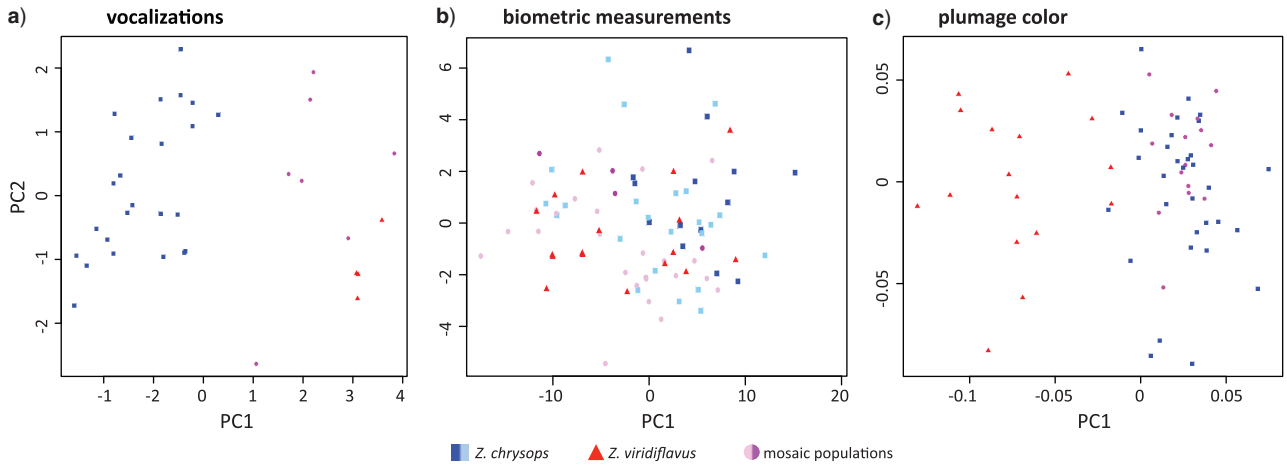

FIGURE 4. Principal component plots of principal component 1 versus principal component 2 for three data sets. Across all three panels, *Z. chrysops* is denoted by squares, *Z. viridiflavus* by triangles, and mosaic birds by circles. Please refer to the color online version for best viewing options of this figure. a) Data set combining 7 vocal parameters for 35 individuals. b) Biometric data (upper mandible, wing, tarsus, and total length) for 91 individuals; for clarity, *Z. chrysops* is divided into Ecuadorian (dark-blue) and Colombian (light sky-blue) populations, whereas mosaic populations are divided into *flavidifrons* (dark-violet) and the unnamed Peruvian population from the departments of SMsA (pinkish-violet). c) Plumage reflectance measurements for 63 individuals.

at http://datadryad.org, doi:10.5061/dryad.633bk). Because all other principal components accounted for only 5.2% of the total variance, we ignored them in subsequent analysis. A PCA plot of vocal data (Fig. 4a) shows that the mosaic birds cluster closely around *Z. viridiflavus* and appear vocally distinct from *Z. chrysops* (for loadings on the first two PCA axes, see Supplementary Table S7, available at http://datadryad.org, doi:10.5061/dryad.633bk).

Bill length was not significantly different between sexes in any of the populations for which a sufficient sample size was available (Supplementary Table S8, available at http://datadryad.org, doi:10.5061/dryad.633bk). In contrast, sex-specific differences in wing, tarsus, and total length were near-significant to highly significant, with increasing significance for higher sample sizes per population (Supplementary Table S8, available at http://datadryad.org, doi:10.5061/dryad.633bk). Hence, wing, tarsus, and total body length, but not bill length, were examined separately for female and male measurements. The different populations and taxa of the *Z. viridiflavus* complex did not cluster discretely in terms of bill, wing, tarsus, and total length in a plot of the first two principal components (Fig. 4b; Supplementary Tables S6 and S7, available at http://datadryad.org, doi:10.5061/dryad.633bk). In pairwise comparisons, there were significant differences in biometric parameters among several taxa. Although bill and tarsus length of mosaic birds differed significantly from both *Z. chrysops* and *Z. viridiflavus* (Supplementary Tables S9 and S10, available at http://datadryad.org, doi:10.5061/dryad.633bk), the only significant differences in wing and total length were between mosaic populations and *Z. chrysops* (Supplementary Tables S11 and S12, available at http://datadryad.org, doi:10.5061/dryad.633bk), especially populations of *Z. chrysops* geographically adjacent to mosaic birds (i.e., those from Ecuador). Note that no comparisons were made between widely allopatric populations, such as between *Z. chrysops* and *Z. viridiflavus*. Consequently, the greatest biometric differences within the *Z. viridiflavus* complex appear to exist between *Z. chrysops* and populations to the south, indicating that mosaic populations more closely resemble their southern neighbor *Z. viridiflavus* in biometric terms.

Despite the great overlap with *Z. viridiflavus* in biometric and vocal characters, the plumage color of mosaic populations was much more similar to *Z. chrysops* (Fig. 4c). In a plot comparing the two leading principal components (explaining ~71.4% of the data) of a plumage reflectance data set of four body parts (Supplementary Tables S6 and S7, available at http://datadryad.org, doi:10.5061/dryad.633bk), mosaic populations were indistinguishable from *Z. chrysops* (Fig. 4c). When the four body parts (belly, breast, crown, and back) were analysed individually among *viridiflavus*, *chrysops*, and the two mosaic groups (*flavidifrons* and the unnamed population from SMsA), inter-taxon comparisons involving *viridiflavus* always revealed color differences that are noticeable or strongly noticeable to the birds' own vision, especially in belly color (Supplementary Table S13, available at http://datadryad.org, doi:10.5061/dryad.633bk). Conversely, comparisons not involving *viridiflavus* revealed substantially less pronounced color differences among taxa (Supplementary Table S13, available at http://datadryad.org, doi:10.5061/dryad.633bk), reflecting traditional ornithological knowledge that *Z. viridiflavus* strongly differs from the other groups in its yellow rather than grayish-white belly.

Downloaded from http://sysbio.oxfordjournals.org/ at Ernst Mayr Library of the Museum Comp Zoology, Harvard University on February 24, 2014

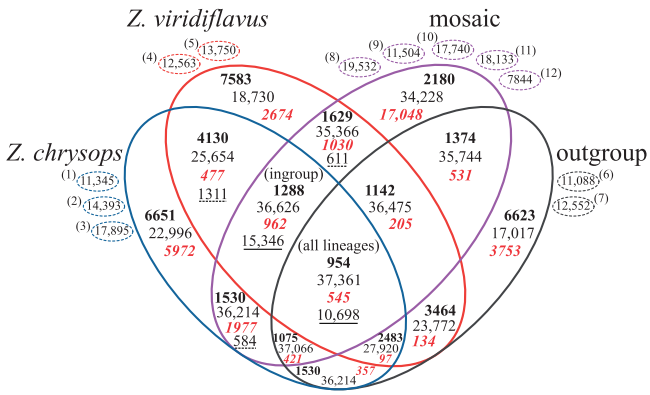

FIGURE 5. Venn diagram of the number of SNP calls and variable loci in the four lineages in our sample. Non-bold, non-italic numbers indicate the number of SNPs called in at least one individual in all lineages encompassing an area. Bold numbers indicate the number of SNPs called in all individuals of all lineages encompassing an area. Bold italic numbers indicate the number of SNPs variable in all and only those lineages encompassing an area (thus, e.g., bold italic numbers in areas contained by only a single lineage represent counts of SNPs private to those lineages, and the number of SNPs variable in all 4 lineages is 545.) Numbers in dashed ovals exterior to the Venn diagram represent the counts of SNPs called in each individual (with the adjacent number indicating the index of the same individual in Supplementary Table S4, available at http://datadryad.org, doi:10.5061/dryad.633bk and Supplementary Fig. S2, available at http://datadryad.org, doi:10.5061/dryad.633bk). In the areas representing all three ingroup lineages and all four lineages, the underlined number is the number of SNPs called in at least one individual per lineage. In the three areas representing pairs of ingroup lineages, the numbers underscored by dashed lines represent the number of contigs containing SNPs called in all individuals represented by the area. These are the sample sizes for the permutation tests for population differentiation adapted from Hudson et al. (1992a, see text).

Population genetic and phylogenetic inferences from genome-wide SNPs

Characteristics of next-generation sequence data.—We obtained a total of 225,325,584 paired-end Illumina reads of 100 bp length each (Supplementary Fig. S2, available at http://datadryad.org, doi:10.5061/dryad.633bk; Supplementary Table S4, available at http://datadryad.org, doi:10.5061/dryad.633bk), amounting to ~22.5 billion bases in total. A total of 1,413,239 sequence contigs made up the PRG (refer to Supplementary Table S14, available at http://datadryad.org, doi:10.5061/dryad.633bk for additional statistics on contig assembly). A total of 37,361 SNPs distributed over 12,721 contigs were called among the 12 individuals (24 chromosomes; Fig. 5), of which 33,069 were variable in the 3 ingroup lineages (Supplementary File 4, available at http://datadryad.org, doi:10.5061/dryad.633bk). For each lineage as well as combinations of different lineages, Figure 5 illustrates the number of SNPs called at least once or across all individuals, while also providing the number of SNPs in which variability is exclusive to certain lineages or lineage combinations. A total of 6736 SNPs were variable within multiple populations/taxa, whereas 29,447 SNPs were variable within only one population/taxon.

Coverage and associated standard deviations for contigs and SNPs were unexpectedly high (contig coverage: mean 24.93; median 9; standard deviation 1602.79; SNP coverage mean 300.58; median 205; standard deviation 460.64). These high values were the result of a number of outlier contigs and SNPs with very high coverage. To test whether these outlier SNPs might affect our analysis, we created a subset (n = 32,103) in which we excluded SNPs whose coverage among called individuals was greater than two standard deviations above the mean. In downstream phylogenetic and population-genetic analyses, results using this subset did not differ substantially from results using the total SNP set (not shown) except for slight differences in the STRUCTURE plots (see below).

Population assignments and divergence.—Genome-wide SNP data indicated that mosaic populations are highly similar to *Z. viridiflavus* (Fig. 6). Using STRUCTURE, the mosaic population was almost entirely assigned to *Z. viridiflavus* when SNP data were attributed to two sources of origin (K=2; Fig. 6a). When three sources of origin were postulated (K=3), mosaic birds did not emerge as an independent population, but instead exhibited genome assignments virtually identical to those shown by *Z. viridiflavus* (Fig. 6b). This result emerged in a data set of all available SNPs polymorphic in the ingroup lineages (n = 33,069; Fig. 6) as well as in three subsets of the latter: (1) all SNPs represented at least once in all four lineages, counting the outgroups as one lineage (n = 8788; graph with near-identical pattern, not shown); (2) all SNPs that mapped to the zebra finch genome (n = 9525; Supplementary Fig. S3, available at http://datadryad.org, doi:10.5061/dryad.633bk); (3) one SNP per contig (n = 11,475; graph with near-identical pattern to Fig. 6, not shown). In the fourth subset, which excluded SNPs of very high coverage (n = 32,103; see above), some mosaic individuals possessed a mixture of ancestry from *Z. viridiflavus* and a third population represented only among mosaic birds (Supplementary Fig. S4, available at http://datadryad.org, doi:10.5061/dryad.633bk). However, mosaic birds were still characterized by a virtual lack of ancestry from *Z. chrysops* and usually shared a majority of their ancestry with *Z. viridiflavus*.

PCA analysis of SNP data also associated the mosaic population with *Z. viridiflavus* and distinguished it from *Z. chrysops* (Fig. 6c). Separation was most pronounced along the first principal component, which accounted for roughly a quarter of the genetic variance captured by PCA (Supplementary Table S6, available at http://datadryad.org, doi:10.5061/dryad.633bk).

The F_{ST}-value between *Z. chrysops* and the mosaic population (F_{ST} = 0.046) was relatively high and comparable to that between *Z. chrysops* and *Z. viridiflavus* (F_{ST} = 0.059; Fig. 6d). In contrast, the F_{ST}-value between the mosaic population and *Z. viridiflavus* (F_{ST} = –0.025) was estimated below zero by the statistic we used (Fig. 6d), essentially indicating a lack of differentiation. Permutation tests for population structure based on

Downloaded from http://sysbio.oxfordjournals.org/ at Ernst Mayr Library of the Museum Comp Zoology, Harvard University on February 24, 2014

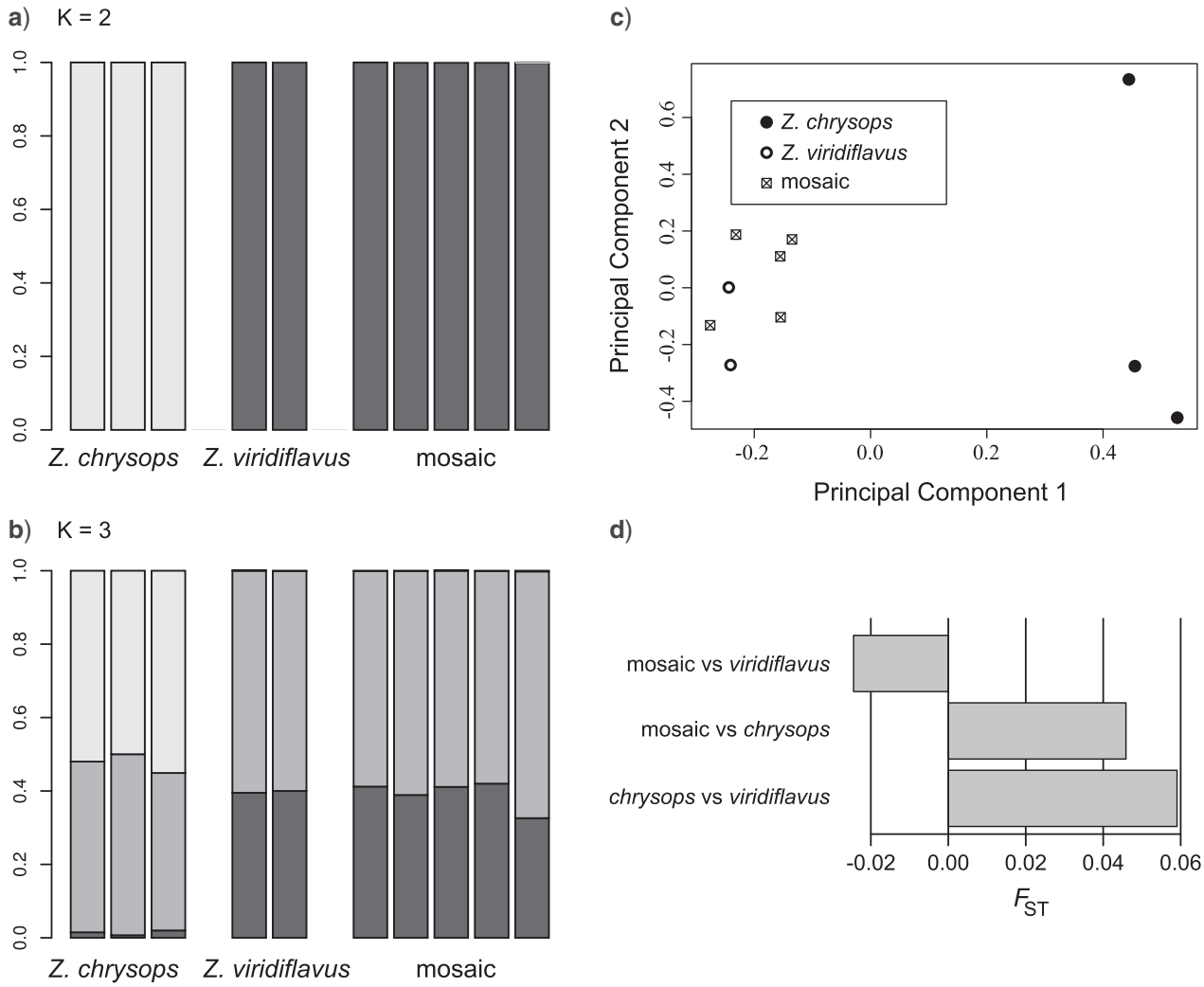

FIGURE 6. a) STRUCTURE plot for 10 ingroup individuals using all available SNPs ($n = 37{,}361$) with $K = 2$, (b) and the same plot with $K = 3$. c) Plots of principal components 1 and 2 in a genome-wide SNP data set ($n = 1288$) for 10 ingroup individuals. (d) Pairwise F_{ST}-values between *Z. viridiflavus*, *Z. chrysops*, and the mosaic population.

K_{ST} showed evidence of structure between *Z. chrysops* and *Z. viridiflavus* ($P < 10^{-6}$) and between the mosaic population and *Z. chrysops* ($P < 10^{-6}$), but not between the mosaic population and *Z. viridiflavus* ($P = 0.08$).

Phylogenetic analysis of SNP data.—SNAPP analyses yielded a species tree topology in which mosaic populations are sister to *Z. viridiflavus* and more distantly related to *Z. chrysops* (Fig. 7a) with maximum branch support. Although this topology and branch lengths remained relatively stable across analyses, our posterior estimates of the population-genetic parameter θ fluctuated with the prior used and was therefore presumably not realistic (Supplementary File 8, available at http://datadryad.org, doi:10.5061/dryad.633bk), which is expected for SNAPP analyses in which there are few internal nodes such as ours (R. Bouckaert, personal communication). When the mosaic population was removed from the data set, the resultant tree showed a deep divergence between *Z. chrysops* and *Z. viridiflavus* with branch length x (a relative measure of substitutions per site) being $0.2 > x > 0.1$ (Fig. 7b). In comparison, divergence between *Z. chrysops* and the mosaic population was much more shallow ($0.1 > x > 0.05$) when *Z. viridiflavus* was removed (Fig. 7c).

The parsimony tree using genotypes in a stepmatrix yielded a topology similar to the SNAPP tree in that *Z. chrysops* was the sister to a lineage that includes *Z. viridiflavus* and mosaic birds (Supplementary Fig. S5, available at http://datadryad.org, doi:10.5061/dryad.633bk). However, there was no high branch support for the monophyly of each of these three lineages. For instance, in the parsimony tree, which uses individuals as operational units rather than populations or taxa as in the SNAPP tree, members of the mosaic population did not emerge as a monophyletic group but clustered paraphyletically around *Z. viridiflavus*.

Downloaded from http://sysbio.oxfordjournals.org/ at Ernst Mayr Library of the Museum Comp Zoology, Harvard University on February 24, 2014

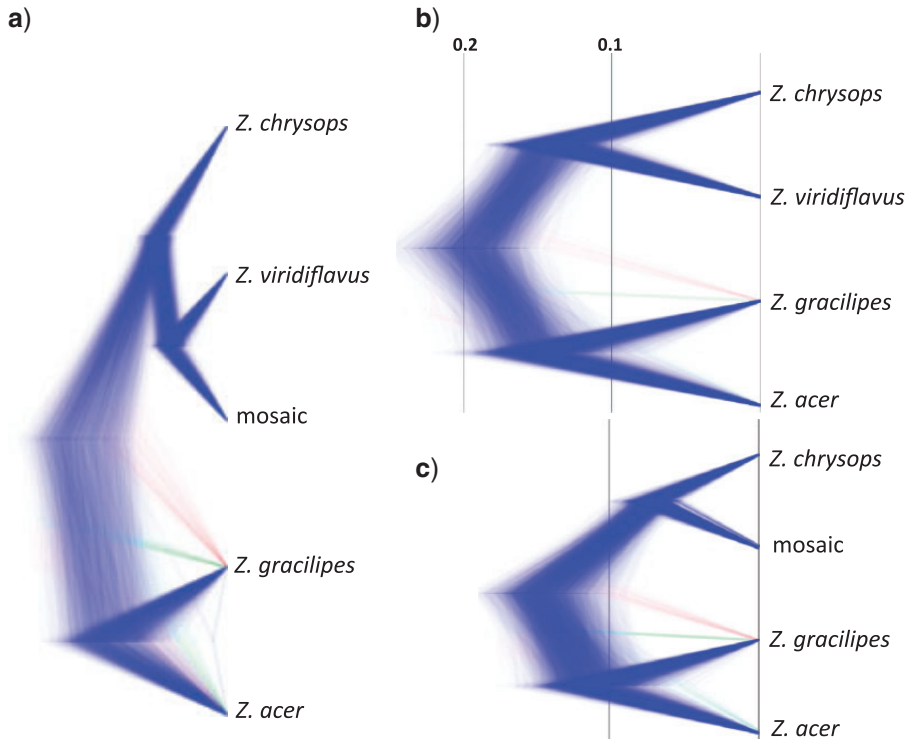

FIGURE 7. Species tree generated by SNAPP analysis (a) for all individuals, (b) under exclusion of the mosaic population, and (c) under exclusion of *Z. viridiflavus*. Branch lengths are a relative measure of substitutions per site. All ingroup nodes are supported by maximum posterior probabilities (pp = 1); monophyly for the two outgroup individuals (*Z. acer* and *Z. gracilipes*) is supported by pp = 0.952 (in panel a), pp = 0.981 (in panel b), and pp = 0.993 (in panel c). For panels (b) and (c) a scale is provided to facilitate branch length comparison. Note: deeper branch lengths between *Z. chrysops* and its sister lineage in (b) as opposed to (c).

Detecting and measuring introgression.—A total of 2710 SNPs across 1537 contigs exhibited the ABBA/BABA pattern required for the detection of genetic introgression with the *D* statistic (Fig. 3). Of these, 535 contigs mapped confidently to the zebra finch genome (Supplementary File 9, available at http://datadryad.org, doi:10.5061/dryad.633bk) and these contigs contained 889 SNPs. Surprisingly, only five of these 889 ABBA–BABA SNPs mapped to the zebra finch Z chromosome, although 22–35 such SNPs mapped to autosomal chromosomes of comparable length, indicating that ABBA–BABA SNPs are substantially under-represented on the Z chromosome (Supplementary Fig. S6, available at http://datadryad.org, doi:10.5061/dryad.633bk). This relationship holds despite the fact that the number of total contigs that mapped against the zebra finch Z chromosome was only about half as high as expected by chromosome length (Supplementary Fig. S6, available at http://datadryad.org, doi:10.5061/dryad.633bk).

Of the 535 contigs mapping to the zebra finch genome, 362 contained either ABBA or BABA-like SNPs but not both (Supplementary Table S15, available at http://datadryad.org, doi:10.5061/dryad.633bk). For the 889 SNP data set, there was a significant preponderance of the ABBA pattern in the data for all linkage block sizes used to carry out the test (*D* = 0.092, range linkage block sizes: 0.2–4 Mb, range jackknife standard error = 0.030–0.34, range *P*-value = 0.0010–0.0033), indicating genetic introgression between *Z. chrysops* and the mosaic population (Fig. 2, hypothesis 1). By considering the probability (calculated using sample allele frequencies) of drawing an ABBA or BABA pattern from the pool of alleles at a given locus, 384 SNPs were classified as ABBA-like and 308 SNPs were classified as BABA-like. The remaining 197 SNPs (out of a total of 889 ABBA/BABA SNPs) produced ABBA and BABA patterns with equal probability.

The mapped contigs on which these SNPs were located were then classified as ABBA-like (n = 204) or BABA-like (n = 158) if they contained only SNPs showing the ABBA or BABA pattern, respectively. Contigs containing both ABBA- and BABA-like SNPs (n = 173) were classified as neither ABBA-like nor BABA-like and were discarded. On an individual level, these classifications are highly influenced by allele-frequency sampling error, but cumulatively—across the group—the ABBA pattern should surface more often in loci experiencing gene flow (Durand et al. 2011).

By maximizing the expression for the admixture fraction in the model of instantaneous admixture (Fig. 3) over a broad and inclusive parameter space (Supplementary Table S5, available at http://datadryad.org, doi:10.5061/dryad.633bk), we found that, at most, ~1.1% of the alleles in the mosaic population had an origin from introgression from *Z. chrysops*. A separate

Downloaded from http://sysbio.oxfordjournals.org/ at Ernst Mayr Library of the Museum Comp Zoology, Harvard University on February 24, 2014

calculation involving the ratio of two unnormalized *D*-statistics showed that a conservative maximum for the fraction of admixture was ~29%. That these two quantities differ so substantially demonstrates the difficulty of calculating an admixture fraction when very little is known about the ancestral population sizes and divergence times of the lineages under consideration. It is possible that this discrepancy is due to errors in the underlying model, particularly the assumptions of instantaneous admixture and the absence of additional gene flow (although these will not affect the interpretation of the *D*-test itself); in any case we interpret this analysis cautiously and note that the small admixture fraction we estimated is also concordant with the results from the STRUCTURE analysis.

Gene ontologies of introgressed alleles.—The putative locations of the 362 mapped contigs (Supplementary Table S15, available at http://datadryad.org, doi:10.5061/dryad.633bk) carrying either ABBA-like SNPs or BABA-like SNPs (but not both) were spread across the zebra finch genome (Fig. 8). The mean distance of the ABBA- and BABA-like SNPs to the nearest annotated gene in the zebra finch genome was 61.6 kb (range 252–495,957 bp); these distances and gene descriptions are given in Supplementary File 9, available at http://datadryad.org, doi:10.5061/dryad.633bk. The Bioconductor tests for GO term enrichment showed no significant enrichment for BABA-linked genes but revealed ten significant associations ($P < 0.05$) between ABBA-linked genes and GO terms associated with cell components (Table 1; Supplementary File 10, available at http://datadryad.org, doi:10.5061/dryad.633bk). The ABBA-linked gene set is significantly enriched for cell component terms that involve cell projection or neuron projection membranes as well as plasma membranes.

Discussion

Phenotypic admixture and gene flow

We compared vocal and phenotypic measurements and generated a genome-wide SNP data set to disentangle an intriguing case of mosaicism among characters in a Neotropical flycatcher complex. We demonstrate that mosaic *Zimmerius* populations are vocally undifferentiated from *Z. viridiflavus*, whereas *Z. chrysops* calls are distinct (Fig. 4a). Plumage reflectance data also confirm previous qualitative assessments that the coloration of mosaic birds is identical or near-identical to *Z. chrysops*, whereas *Z. viridiflavus* looks distinctly different (Fig. 4c), particularly in its belly color (Supplementary Table S13, available at http://datadryad.org, doi:10.5061/dryad.633bk), which has long been known to be distinct in *viridiflavus* compared with the other *Zimmerius* taxa and populations (Ridgely and Tudor 1994; Schulenberg et al. 2007). Across mensural characters, there is large overlap among populations (Fig. 4b). However, when only wing and total length are considered, significant

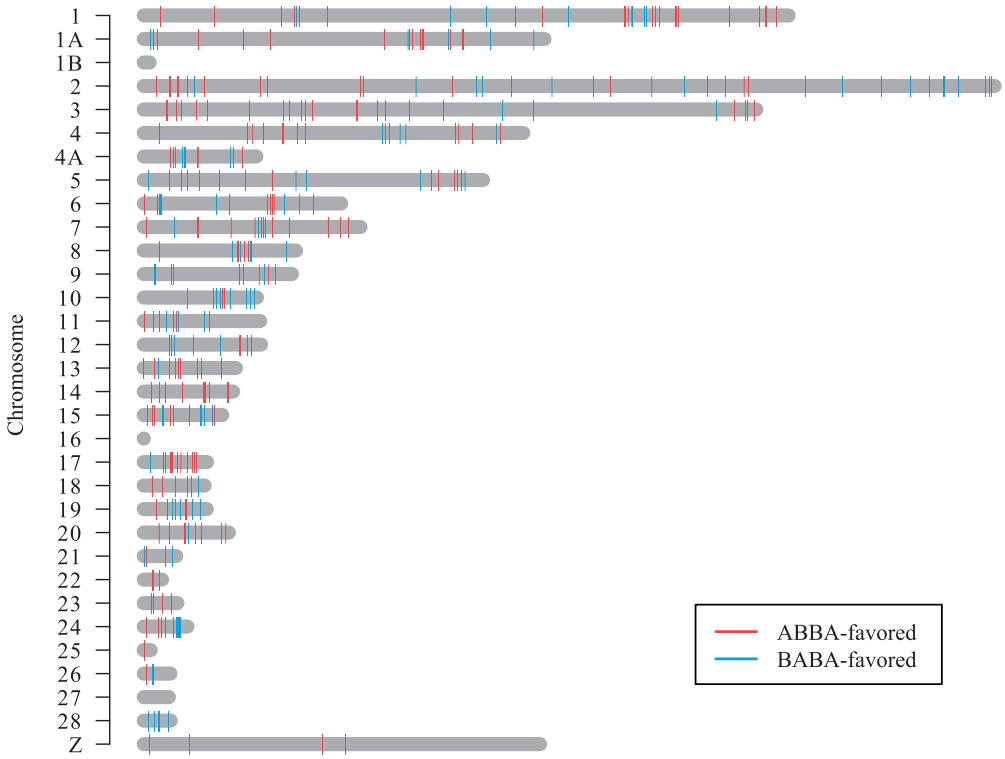

FIGURE 8. Chromosomal positions of ABBA- and BABA-like sites mapped onto the zebra finch genome.

Downloaded from http://sysbio.oxfordjournals.org/ at Ernst Mayr Library of the Museum Comp Zoology, Harvard University on February 24, 2014

TABLE 1. Summary of the over-represented GO terms; all GO terms were in the category "cellular components"

GO identification number	GO term	Annotated	Significant	Expected	Corrected
GO:0031253	Cell projection membrane	53	7	0.59	0.00186
GO:0042995	Cell projection	485	17	5.38	0.01074
GO:0005886	Plasma membrane	1407	32	15.6	0.01074
GO:0016020	Membrane	3985	65	44.17	0.01074
GO:0044459	Plasma membrane part	736	21	8.16	0.01074
GO:0032589	Neuron projection membrane	8	3	0.09	0.01206
GO:0071944	Cell periphery	1460	32	16.18	0.01206
GO:0044463	Cell projection part	208	10	2.31	0.01370
GO:0031256	Leading edge membrane	27	4	0.3	0.02557
GO:0044425	Membrane part	2740	47	30.37	0.04932

The following abbreviations are used: annotated, number of zebra finch genes the GO term is annotated to; significant, number of ABBA-linked genes the GO term is annotated to; expected, number of ABBA-linked genes the GO term would be expected to be annotated to; corrected, the significance level from the Fisher's exact test (*P*-value) after correcting for multiple tests with FDR <0.05.

differences are consistently found between mosaic birds and adjacent populations of *Z. chrysops* (Supplementary Tables S11 and S12, available at http://datadryad.org, doi:10.5061/dryad.633bk).

Plumage coloration was used in the past to erroneously classify mosaic populations as members of *Z. chrysops* at a time when their vocal, biometric, and mitochondrial affinity with *Z. viridiflavus* was unknown (Ridgely and Tudor 1994; Fitzpatrick 2004). In contrast to the previous plumage-based classification, mosaic birds emerge as virtually indistinguishable from *Z. viridiflavus* but distinct from *Z. chrysops* (Fig. 6) in various SNP analyses (STRUCTURE plots and PCA), supporting mtDNA and vocal results that suggest conspecificity with *Z. viridiflavus*, not *Z. chrysops* (Rheindt et al. 2008a). Measures of population differentiation, such as F_{ST} (Fig. 6d) and Hudson et al.'s (1992a) permutation test, also reject a scenario in which mosaic populations form an additional anciently diverged evolutionary lineage. Thus our population-genetic analyses strongly support hypothesis 1 or hypothesis 5 (Fig. 2), in which mosaic birds are conspecific with southern *Z. viridiflavus*. Additionally, we estimated a species tree and a parsimony tree in which mosaic birds are more closely related to *Z. viridiflavus* (Fig. 7a, Supplementary Fig. S5, available at http://datadryad.org, doi:10.5061/dryad.633bk). In summary, the large bulk of genomic variation in mosaic birds is shared with *Z. viridiflavus*.

We suggest that hypotheses 2, 3, and 4 (Fig. 2) provide a less likely explanation of our data. If mosaic birds did not belong to *Z. viridiflavus* but to *Z. chrysops*, or if they constituted an old species-level lineage of their own or a genomic mix of both species, one would not expect them to share the large bulk of genomic variation with *Z. viridiflavus*. However, not only do mosaic birds share their genomic make-up with *Z. viridiflavus*, but they are also virtually identical or extremely similar to *Z. viridiflavus* across many traits (bioacoustic, biometric), with only one trait (belly color) linking them to *Z. chrysops*.

When mosaic birds are removed from the data set, the resulting species tree exhibits a deep divergence between *Z. chrysops* and *Z. viridiflavus* relative to the more shallow divergence between *Z. chrysops* and the mosaic population when *Z. viridiflavus* is removed (Fig. 7b,c), suggesting that introgression between *Z. chrysops* and mosaic birds may be at play. The ABBA/BABA test also suggested cryptic gene flow between *Z. chrysops* and the mosaic population. Without additional information, this test is unable to discern the direction of gene flow between these two taxa. Even so, the data are consistent with a scenario in which mosaic birds and northern *Z. chrysops* have recently engaged in inter-specific gene flow with each other. Given the evidence for gene flow between them and the fact that the two populations are geographically adjacent, we believe our data are most consistent with a scenario in which the white belly color of the mosaic population arose via gene flow from *Z. chrysops* (Fig. 2, hypothesis 1;. The demonstration of a functional link between introgression and belly color in future studies (see below) is desirable to fully rule out chance convergence (Fig. 2, hypothesis 5).

Slatkin and Pollack (2008) suggested that a strong data signal for phylogenetic tree topologies other than the species tree topology may be due to population subdivision in the ancestral species. In the context of *Zimmerius* flycatchers, this means that a preponderance of ABBA-like SNPs may not be due to recent gene flow (i.e., introgression) but due to ancient subdivision in the ancestral species that would have entailed regular gene flow between the populations that gave rise to *Z. chrysops* and mosaic birds, but reduced gene flow toward populations that gave rise to *Z. viridiflavus* (Supplementary Fig. S7, available at http://datadryad.org, doi:10.5061/dryad.633bk). Slatkin and Pollack's (2008) results are a reminder of caution when basing the diagnosis of genetic introgression solely on ABBA–BABA test results. However, Slatkin and Pollack (2008) show that substantial levels of persistent ancestral subdivision are needed to account for such patterns of asymmetry of tree signal. Elaeniine tyrant-flycatchers (Elaeniinae)—to which the genus *Zimmerius* belongs—are known to have undergone a turbulent Pleistocene and late Pliocene evolutionary history, especially those species

Downloaded from http://sysbio.oxfordjournals.org/ at Ernst Mayr Library of the Museum Comp Zoology, Harvard University on February 24, 2014

that live in Andean forest habitats subject to continual climatic fluctuations and distributional shifts (Rheindt et al. 2008c, 2009b). Andean cloud forests are a highly fragmented environment that has undergone dramatic shifts and fluctuations in extent throughout the glacial cycles of the last 3 million years. It is unlikely that Andean cloud forests could have provided a suitable setting for Slatkin and Pollack's (2008) requirement for persistent ancestral subdivision lasting beyond speciation events (Supplementary Fig. S7, available at http://datadryad.org, doi:10.5061/dryad.633bk). Hence, introgression remains the most plausible explanation for our ABBA–BABA test results. Extensions of the ABBA/BABA test (Eaton and Ree 2013) and additional taxon sampling may allow us to discriminate between these hypotheses and to more finely estimate the contribution of introgression to different populations in the complex.

Low levels of introgression associated with plumage assimilation

Genetic introgression may lead to a phenotypic assimilation of admixed individuals toward the donor population, as commonly happens in avian hybrid zones (see Rheindt and Edwards 2011 for an overview). However, there is a scarcity of data on whether phenotypic changes are accompanied by equivalent levels of genetic introgression. Our study documents a likely case of phenotypic admixture characterized by low levels of genetic introgression. Although the phenotypically admixed individuals are virtually pure in terms of mtDNA and nuclear DNA, their plumage is identical to a neighboring species to the north. If, as we suggest, the yellow versus white belly coloration in the Z. viridiflavus complex is due to carotenoid, not melanin, pigmentation (McGraw 2006), then we may have found functional links between putatively introgressed loci and plumage coloration in this complex. There is limited knowledge on the mechanisms of carotenoid coloration in birds (McGraw 2004; Walsh et al. 2012). In principle, the low level of introgression may affect key loci responsible for carotenoid pigmentation, although our data do not provide any direct evidence for this. However, we were surprised to find that the ABBA-favored SNPs suggesting gene flow between *chrysops* and the mosaic birds were close to genes that were enriched for functions in cell projection or neuron projection membranes and in plasma membranes (Table 1; Supplementary Table S15, available at http://datadryad.org, doi:10.5061/dryad.633bk). Significant enrichment for specific GO terms in any data set does not necessarily suggest strong functional links with the particular phenotype under consideration. Still, the connection between plumage coloration and cell membranes may not be as far fetched as it sounds. As mentioned earlier, the yellow–white coloration difference among *Zimmerius* taxa is possibly dependent on carotenoid pigments, which are delivered through the bloodstream to generate metabolically derived body colorants directly at the site of feather growth (McGraw 2004). Although our knowledge about the carotenoid pathway is still meager, Walsh et al. (2012) present a list of candidate genes for carotenoid pigmentation, several of which are transporters bound to cell membranes and involved in the uptake of carotenoids.

In the end, many of the SNPs in our enrichment analysis are far enough from the closest genes to become effectively unlinked to them, particularly if population sizes and the population recombination rate are large, which is the case for many natural bird populations (Edwards and Smith 2004; Balakrishnan and Edwards 2009; Backström et al. 2013). Thus our finding of significant GO enrichment may be entirely spurious. Still, the potential association of ABBA-linked introgressed genes in this complex with carotenoid pigmentation and belly coloration needs further exploration, and future studies of plumage assimilation should closely examine loci potentially involved in the carotenoid synthesis pathway (Walsh et al. 2012). It is possible that the introgression of plumage alleles between the mosaic and *chrysops* populations has been aided by selection (Seehausen 2004; Nolte et al. 2009; Grant and Grant 2010; Gompert et al. 2012; Staubach et al. 2012), although our data cannot distinguish this scenario from a neutral one.

ABBA/BABA-like SNPs and the Z chromosome

In our data set, the number of contigs that mapped against the zebra finch Z chromosome was only about half as high as expected by chromosome length (Supplementary Fig. S6a, available at http://datadryad.org, doi:10.5061/dryad.633bk). This under-representation may be due to the lower effective population size of the Z chromosome. In birds, females carry one copy of the Z chromosome whereas males carry two. The lower number of Z copies (compared with copies of autosomal loci) may translate into a lower level of genetic variation that has accumulated in the birds' evolutionary history. This sexual imbalance in the number of Z locus copies may have had a significant impact on our results because 40% of our ingroup individuals were female (Supplementary Table S4, available at http://datadryad.org, doi:10.5061/dryad.633bk). In female samples, the volume of Z-chromosomal DNA would have been under-represented in the starting DNA, and Z-linked reads may have had a higher chance of falling below our quality thresholds for sequence coverage, leading to a reduced number of Z-associated contigs.

We detected a shortage of ABBA–BABA sites mapping against the zebra finch Z chromosome versus autosomal chromosomes of comparable length. This shortage cannot be explained by the general under-representation of Z contigs in our data set (Supplementary Fig. S6b–d, available at http://datadryad.org, doi:10.5061/dryad.633bk). This finding indicates that ABBA–BABA sites in our data

Downloaded from http://sysbio.oxfordjournals.org/ at Ernst Mayr Library of the Museum Comp Zoology, Harvard University on February 24, 2014

set are more rarely found in the Z chromosome than expected. An explanation for the relatively low number of ABBA–BABA sites on the Z chromosome is that these loci may be subject to frequent selective sweeps, wiping away shared polymorphisms and hence both ABBA and BABA sites (Carling et al. 2010).

Genome-wide SNP sampling and reconstructing evolutionary history

Using the RAD-seq approach, we generated a data set of 37,361 genome-wide SNPs. Of these, 33,069 SNPs (88.5%) were variable within the ingroup samples and were used in STRUCTURE analyses (Fig. 6a,b), confirming the validity of the RAD-seq approach for population-genetic inquiries. Our recovery of orthologous SNPs across populations was much lower than the total number of SNP loci recovered, which can affect methods sensitive to missing data. For instance, SMARTPCA analysis was based on only 1288 variable SNPs (3.9%) that had been called in all ingroup individuals (Fig. 6c), whereas the SNAPP tree was based on 954 variable SNPs (2.9%), that is those called in all individuals (Fig. 7). However, the volume of even these restricted subsets of the data still compares favorably to traditional population genetic and phylogenetic studies in birds. The key advance that RAD-seq has provided for our study system is the generation of SNPs spaced throughout the genome. In truth, the largest phylogeographic studies in terms of loci sampled in birds (Lee and Edwards 2008; Balakrishnan and Edwards 2009) and other groups (e.g., O'Neill et al. 2013) using PCR or hybrid PCR/next-generation methods yielded data sets with a comparable number of SNPs (e.g., Lee and Edwards [2008], 1575 autosomal SNPs in total with the red-backed fairy wren *Malurus melanocephalus*; O'Neill et al. (2013), 2627 SNPs in the salamander *Ambystoma tigrinum*). However, in these studies, the SNPs were distributed among a smaller subset of loci (e.g., 36 loci for fairy wrens, 94 loci in salamanders), yielding what is likely a much smaller subset of effectively independent SNPs. Thus, our study yielded a set of genetically independent SNPs that is likely much larger than these PCR-based studies. Still, given these numbers, greater coverage of all individuals in our study would have increased the number of loci we could apply to any particular test or statistic (e.g. McCormack et al. 2012). The number of SNPs we studied was great enough to discern key aspects of the demographic history of this group, yet it is unclear whether a larger number of SNPs would have increased resolution of the relatively simple demographic scenarios we tested.

To the best of our knowledge, ours may be the first application of SNAPP, a species tree method that relies solely on SNPs—apart from the inventors' initial applications (Bryant et al. 2012). The resultant species tree's topology and branch lengths are similar to a parsimony tree using all SNPs (Fig. 7; Supplementary Fig. S5, available at http://datadryad.org, doi:10.5061/dryad.633bk), suggesting that SNAPP returns trees that conform well to expectations from more traditional tree analyses. SNAPP makes the explicit assumption of zero gene flow between species-level lineages such that any signal discordance between SNPs is interpreted as incomplete lineage sorting. Although SNAPP is not designed for evolutionary scenarios in which introgression is suspected, it may perform well in cases like ours where the contribution by introgression is estimated to be limited. Although it was comforting that the parsimony tree yielded topologies consistent with the SNAPP tree, it is important to point out that the logic of this tree is inherently flawed because of the use of individuals as operational units. Individuals within and between species are not related to one another hierarchically, but rather as part of complex pedigrees, thus representing diploid individuals (genotypes) on a tree is a crude approximation of the true history.

Our analyses suggest that genome-wide SNP data sets are needed to detect low levels of gene flow, such as the kind of genetic introgression leading to allele exchange at a small subset of the genome. Although genetic introgression has been studied for many decades, new breakthroughs in our knowledge of introgression have recently been achieved, partly because of the development of new tests to detect it (Green et al. 2010; Durand et al. 2011), and partly because low levels of introgression would escape traditional sequencing methods that only target a limited number of loci. In our study, only 2710 of total SNPs (7.3%) exhibited the ABBA–BABA pattern that lends itself to the detection of introgression using this test, and we only had linkage information for 889 of those (2.4%). This latter number of SNPs sufficed for detecting limited introgression between mosaic birds and *Z. chrysops*. The value of the D statistic we estimated is similar to values obtained for introgression from Neanderthals ($0.039 < D < 0.053$) or other archaic humans ($0.040 < D < 0.091$) into some groups of modern humans (Green et al. 2010; Reich et al. 2010).

Our study confirms the findings of previous studies on hominids (Green et al. 2010; Reich et al. 2010) that patterns of introgression can be detected in data sets with few individuals. However, distinguishing between more elaborate scenarios of one-time or repeated introgression and establishing introgression directionality in future studies will likely require data sets with a greater individual sample size, both from within populations and especially across geographic areas, as well as increased SNP yields. Novel laboratory protocols (e.g., Peterson et al. 2012) are already allowing researchers to increase the number of individuals and sequence yield per sequencing run in next-generation applications that are based on reduced-representation libraries such as RAD-seq. With a further reduction in prices, whole-genome resequencing may soon become an option for phylogeneticists and population geneticists eager to increase sequence yield for probing ever deeper into the processes that have shaped populations.

Downloaded from http://sysbio.oxfordjournals.org/ at Ernst Mayr Library of the Museum Comp Zoology, Harvard University on February 24, 2014

Supplementary Material

Data files and/or other supplementary information related to this article have been deposited at http://datadryad.org/ under the doi:10.5061/dryad.633bk. The original raw Illumina reads have been uploaded to Genbank's SRA (study accession number: SRP030706). The PRG contigs fasta file and SNP pileup file form an additional part of our Dryad submission.

Funding

This work was supported by National Science Foundation (NSF) [DEB–0743616 to S.V.E. and DBI-0905714 to M.K.F.] and funds from the Museum of Comparative Zoology, Harvard University; a postdoctoral fellowship granted by the Deutsche Akademische Austauschdienst (DAAD) (to F.E.R.); and National University of Singapore (NUS) Faculty of Science start-up [WBS R-154-000-570-133 to F.E.R.].

Acknowledgements

We thank Rafael Maia and Allison Shultz for their kind help with spectrophotometric analysis, and Rafael Maia for helpful discussion on appropriate ways of comparing coloration measurements. We thank Qu Zhang for providing an R script for carrying out the Bioconductor analysis. We had helpful discussions with Mike Sorenson and his lab in the early phases of this project. We are indebted to Jonathan Losos, Yoel Stuart, and Nicholas Crawford for the use of a spectrophotometer. Remco Bouckaert is acknowledged for helpful discussion on SNAPP. Claire Reardon and Chris Daily provided advice and assistance with the application of Illumina sequencing. Nick Patterson engaged in extremely helpful discussions about the use of the D statistic. Ryan Chisholm helped address a reviewer concern about vocal analysis. We thank Robb Brumfield, Van Remsen, and Donna Dittmann at the Louisiana State University Museum of Natural Science for their generous tissue loan and Leo Joseph and Nate Rice (Academy of Natural Sciences, Philadelphia) for complementary tissue for one individual. We thank Darren Irwin, Brant Faircloth, John McCormack, and Frank Anderson for extremely helpful comments that assisted in the improvement of the original manuscript.

References

Anderson T.M., vonHoldt B.M., Candille S.I., Musiani M., Greco C., Stahler D.R., Smith D.W., Padhukasahasram B., Randi E., Leonard, J.A., Bustamante C.D., Ostrander E.A., Tang H., Wayne R.K., Barsh G.S. 2009. Molecular and evolutionary history of melanism in North American gray wolves. Science 323:1339–1343.

Arnold B., Corbett-Detig R.B., Hartl D., Bomblies K. 2013. RADseq underestimates diversity and introduces genealogical biases due to nonrandom haplotype sampling. Mol. Ecol. 22:3179–3190.

Backström N., Shipilina D., Blom M.P.K., Edwards S.V. 2013. Cis-regulatory sequence variation and association with *Mycoplasma* load in natural populations of the house finch (*Carpodacus mexicanus*). Ecol. Evol. 3:655–666.

Balakrishnan C.B., Edwards S.V. 2009. Nucleotide variation, linkage disequilibrium and founder-facilitated speciation in wild populations of the zebra finch (Taeniopygia guttata). Genetics 181:645–660.

Barker D.L., Hansen M.S.T., Faruqi A.F., Giannola D., Irsula O.R., Lasken R.S., Latterich M., Makarov V., Oliphant A., Pinter J.H., Shen R., Sleptsova I., Ziehler W., Lai E. 2004. Two methods of whole-genome amplification enable accurate genotyping across a 2320-SNP linkage panel. Genome Res. 14:901–907.

Benites P., Eaton M.D., Lijtmaer D.A., Lougheed S.C., Tubaro P.L. 2010. Analysis from avian visual perspective reveals plumage colour differences among females of capuchino seedeaters (*Sporophila*). J. Avian Biol. 41:597–602.

Bers N.E.M.V., Oers K.V., Kerstens H.H.D., Dibbits B.W., Crooijmans R.P.M.A., Visser M.E., Groenen M.A.M. 2010. Genome-wide SNP detection in the great tit *Parus major* using high throughput sequencing. Mol. Ecol. 19:89–99.

Bioacoustics Research Program. 2011. Raven Pro: interactive sound analysis software (Version 1.4). Ithaca: The Cornell Lab of Ornithology. Available from: URL http://www.birds.cornell.edu/raven.

Bouckaert R.R. 2010. DensiTree: making sense of sets of phylogenetic trees. Bioinformatics 26:1372–1373.

Bryant D., Bouckaert R., Felsenstein J., Rosenberg N.A., RoyChoudhury A. 2012. Inferring species trees directly from biallelic genetic markers: bypassing gene trees in a full coalescent analysis. Mol. Biol. Evol. 29:1917–1932.

Carling M.D., Brumfield R.T. 2007. Gene sampling strategies for multi-locus population estimates of genetic diversity (θ). PLoS ONE 2(1):e160.

Carling M.D., Lovette I.J., Brumfield R.T. 2010. Historical divergence and gene flow: coalescent analyses of mitochondrial, autosomal, and sex-linked loci in *Passerina* buntings. Evolution 64:1762–1772.

Cibois A., Thibault J.-C., Pasquet E. 2012. The molecular basis of the plumage colour polymorphism in the Tahiti reed-warbler *Acrocephalus caffer*. J. Avian Biol. 43:3–8.

Currat M., Ruedi M., Petit R.J., Excoffier L. 2008. The hidden side of invasions: massive introgression by local genes. Evolution 62:1908–1920.

Darwin C. 1859. On the origin of species by means of natural selection. London: John Murray.

Doucet S.M., Shawkey M.D., Rathburn M.K., Mays H.L., Montgomerie R. 2004. Concordant evolution of plumage colour, feather microstructure and a melanocortin receptor gene between mainland and island populations of a fairy-wren. P. Roy. Soc. B Biol. Sci. 271:1663–1670.

Durand E.Y., Patterson N., Reich D., Slatkin M. 2011. Testing for ancient admixture between closely related populations. Mol. Biol. Evol. 28:2239–2252.

Eaton M.D. 2005. Human vision fails to distinguish widespread sexual dichromatism among sexually "monochromatic" birds. P. Natl Acad. Sci. USA 102:10942–10946.

Eaton D.A.R, Ree R.H. 2013. Inferring phylogeny and introgression using RADseq data: an example from flowering plants (*Pedicularis*: Orobanchaceae). Syst. Biol. 62:689–706.

Edwards S.V. 2009. Is a new and general theory of systematics emerging? Evolution 63:1–19.

Edwards S.V., Smith M. 2004. Hitchhiking and recombination in birds: evidence from Mhc-linked and unlinked loci in red-winged blackbirds (*Agelaius phoeniceus*). Genet. Res. 84:175–192.

Ellegren H. 2010. Evolutionary stasis: the stable chromosomes of birds. Trends Ecol. Evol. 25:283–291.

Feder J.L., Egan S.P., Nosil P. 2012. The genomics of speciation-with-gene-flow. Trends Genet. 28:342–350.

Felsenstein J. 2006. Accuracy of coalescent likelihood estimates: do we need more sites, more sequences, or more loci? Mol. Biol. Evol. 23:691–700.

Fitzpatrick J.W. 2004. Family Tyrannidae (tyrant-flycatchers). In: del Hoyo J., Elliott A., Christie D.A., editors. Handbook of the birds of

Downloaded from http://sysbio.oxfordjournals.org/ at Ernst Mayr Library of the Museum Comp Zoology, Harvard University on February 24, 2014

the world, cotingas to pipits and wagtails. Vol. 9. Barcelona: Lynx Edicions. p. 170–464.
Fuchs J., Pons J.M., Liu L., Ericson P.G., Couloux A., Pasquet E. 2013. A multi-locus phylogeny suggests an ancient hybridization event between *Campephilus* and melanerpine woodpeckers (Aves: Picidae). Mol. Phylogenet. Evol. 67:578–588.
Garrigan D., Hammer M.F. 2006. Reconstructing human origins in the genomic era. Nat. Rev. Genet. 7:669–680.
Gompert Z., Lucas L.K., Nice C.C., Fordyce J.A., Forister M.L., Buerkle C.A. 2012. Genomic regions with a history of divergent selection affect fitness of hybrids between two butterfly species. Evolution 66:2167–2181.
Grant P.R., Grant B.R. 2010. Conspecific versus heterospecific gene exchange between populations of Darwin's finches. Philos. T. R. Soc. Lond. B 365:1065–1076.
Green R.E., Krause J., Briggs A.W., Maricic T., Stenzel U., Kircher M., Patterson N., Li H., Zhai W., Fritz M.H.-Y., Hansen N.F., Durand E.Y., Malaspinas A.-S., Jensen J.D., Marques-Bonet T., Alkan C., Prüfer K., Meyer M., Burbano H.A., Good J.M., Schultz R., Aximu-Petri A., Butthof A., Höber B., Höffner B., Siegemund M., Weihmann A., Nusbaum C., Lander E.S., Russ C., Novod N., Affourtit J., Egholm M., Verna C., Rudan P., Brajkovic D., Kucan Z., Gusic I., Doronichev V.B., Golovanova L.V., Lalueza-Fox C., de La Rasilla M., Fortea J., Rosas A., Schmitz R.W., Johnson P.L.F., Eichler E.E., Falush D., Birney E., Mullikin J.C., Slatkin M., Nielsen R., Kelso J., Lachmann M., Reich D., S. Pääbo. 2010. A draft sequence of the Neandertal genome. Science 328:710–722.
Gronau I., Hubisz M.J., Gulko B., Danko C.G., Siepel A. 2011. Bayesian inference of ancient human demography from individual genome sequences. Nat. Genet. 43:1031–1034.
Han T., Chang C.-W., Kwekel J.C., Chen Y., Ge Y., Martinez-Murillo F., Roscoe D., Težak Ž., Philip R., Bijwaard K., Fuscoe J.C. 2012. Characterization of whole genome amplified (WGA) DNA for use in genotyping assay development. BMC Genomics 13:217.
Hart N.S., Hunt D.M. 2007. Avian visual pigments: characteristics, spectral tuning, and evolution. Am. Nat. 169:s7–s27.
Hudson R.R. 2002. Generating samples under a Wright-Fisher neutral model. Bioinformatics 18:337–338.
Hudson R.R., Boos D.D., Kaplan N.L. 1992a. A statistical test for detecting geographic subdivision. Mol. Biol. Evol. 9:138–151.
Hudson R.R., Slatkin M., Maddison W.P. 1992b. Estimation of levels of gene flow from DNA sequence data. Genetics 132:583–589.
Isler M.L., Isler P.R., Whitney B.M. 1998. Use of vocalizations to establish species limits in antbirds (Passeriformes: Thamnophilidae). Auk 115:577–590.
Koboldt D., Zhang Q., Larson D., Shen D., McLellan M., Lin L., Miller C., Mardis E., Ding L., Wilson R. 2012. VarScan 2: somatic mutation and copy number alteration discovery in cancer by exome sequencing. Genome Res. 22:568–576.
Kroodsma D.E., Konishi M. 1991. A suboscine bird (eastern phoebe, *Sayornis phoebe*) develops normal song without auditory feedback. Anim. Behav. 42:477–487.
Kulathinal R.J., Stevison L.S., Noor M.A.F. 2009. The genomics of speciation in *Drosophila*: diversity, divergence, and introgression estimated using low-coverage genome sequencing. PLoS Genet. 5:e1000550.
Lee J.Y., Edwards S.V. 2008. Divergence across Australia's Carpentarian barrier: statistical phylogeography of the red-backed fairy wren (*Malurus melanocephalus*). Evolution 62:3117–3134.
Li H., Durbin R. 2011. Inference of human population history from individual whole-genome sequences. Nature 475:493–496.
Li H., Durbin R. 2009. Fast and accurate short read alignment with Burrows-Wheeler Transform. Bioinformatics 25:1754–1760.
Mallet J. 2005. Hybridization as an invasion of the genome. Trends Ecol. Evol. 20:229–237.
Martin E.R., Kinnamon D.D., Schmidt M.A., Powell E.H., Zuchner S., Morris R.W. 2010. SeqEM: an adaptive genotype-calling approach for next-generation sequencing studies. Bioinformatics 26:2803–2810.
Mayr E. 1963. Animal species and evolution. Cambridge (MA): Harvard University Press.
McCormack J.E., Venkatraman M.X. 2013. A distinctive genetic footprint of ancient hybridization. Auk 130:469-475.
McCormack J.E., Maley J.M., Hird S.M., Derryberry E.P., Graves G.R., Brumfield R.T. 2012. Next-generation sequencing reveals phylogeographic structure and a species tree for recent bird divergences. Mol. Phylogenet. Evol. 62:397–406.
McGraw K.J. 2006. Mechanics of carotenoid-based coloration. In: Hill G.E., McGraw K., editors. Bird coloration, vol. I. mechanisms and measurements. Cambridge: Harvard University Press. p. 177–242.
McGraw K.J. 2004. Colorful songbirds metabolize carotenoids at the integument. J. Avian Biol. 35:471–476.
McGraw K.J., Hill G.E. 2000. Carotenoid-based ornamentation and status signaling in the house finch. Behav. Ecol. 11:520–527.
Mundy N.I., Badcock N.S., Hart T., Scribner K., Janssen K., Nadeau N.J. 2004. Conserved genetic basis of a quantitative plumage trait involved in mate choice. Science 303:1870–1873.
Nolte A.W., Tautz D. 2010. Understanding the onset of hybrid speciation. Trends Genet. 26:54–58.
Nolte A.W., Gompert Z., Buerkle C.A. 2009. Variable patterns of introgression in two sculpin hybrid zones suggest that genomic isolation di?ers among populations. Mol. Ecol. 18:2615–2627.
O'Neill E.M., Schwartz R., Bullock C.T., Williams J.S., Shaffer H.B., Aguilar-Miguel X., Parra-Olea G., Weisrock D.W. 2013. Parallel tagged amplicon sequencing reveals major lineages and phylogenetic structure in the North American tiger salamander (*Ambystoma tigrinum*) species complex. Mol. Ecol. 22:111–129.
Osorio D., Smith A.C., Vorobyev M., Buchanan-Smith H.M. 2004. Detection of fruit and the selection of primate visual pigments for color vision. Am. Nat. 164:696–708.
Patterson N., Price A.L., Reich D. 2006. Population structure and eigenanalysis. PLoS Genet. 2:e190.
Peterson B.K., Weber J.N., Kay E.H., Fisher H.S., Hoekstra H.E. 2012. Double digest RADseq: an inexpensive method for *de novo* SNP discovery and genotyping in model and non-model species. PLoS ONE 7(5):e37135.
Pritchard J.K., Stephens M., Donnelly P. 2000. Inference of population structure using multilocus genotype data. Genetics 155:945–959.
R Development Core Team. 2008. R: a language and environment for statistical computing Vienna: R Foundation for Statistical Computing.
Rambaut A., Drummond A.J. 2007. Tracer v1.4. Available from: URL http://beast.bio.ed.ac.uk/Tracer.
Reich D., Green R.E., Kircher M., Krause J., Patterson N., Durand E.Y., Viola B., Briggs A.W., Stenzel U., Johnson P.L.F., Maricic T., Good J.M., Marqués-Bonet T., Alkan C., Fu Q., Mallick S., Li H., Meyer M., Eichler E.E., Stoneking M., Richards M., Talamo S., Shunkov M.V., Derevianko A.P., Hublin J.-J., Kelso J., Slatkin M., Pääbo S. 2010. Genetic history of an archaic hominin group from Denisova Cave in Siberia. Nature 468:1053–1060.
Reich D., Thangaraj K., Patterson N., Price A.L., Singh L. 2009. Reconstructing Indian population history. Nature 461:489–494.
Rheindt F.E., Edwards S.V. 2011. Genetic introgression: an integral but neglected component of speciation in birds. Auk 128:620–632.
Rheindt F.E., Christidis L., Norman J.A. 2009a. Genetic introgression, incomplete lineage sorting and faulty taxonomy create multiple cases of polyphyly in a montane clade of tyrant-flycatchers (*Elaenia*, Tyrannidae). Zool. Scr. 38:143–153.
Rheindt F.E., Christidis L., Cabanne G.S., Miyaki C., Norman J.A. 2009b. The timing of Neotropical speciation dynamics in the late Neogene: a reconstruction of *Myiopagis* flycatcher diversification using phylogenetic and paleogeographic data. Mol. Phylogenet. Evol. 53:961–971.
Rheindt F.E., Norman J.A., Christidis L. 2008a. DNA evidence shows vocalizations to be a better indicator of taxonomic limits than plumage patterns in *Zimmerius* tyrant-flycatchers. Mol. Phylogenet. Evol. 48:150–156.
Rheindt F.E., Norman J.A., Christidis L. 2008b. Phylogenetic relationships of tyrant-flycatchers (Aves; Tyrannidae), with an emphasis on the elaeniine assemblage. Mol. Phylogenet. Evol. 46:88–101.
Rheindt F.E., Christidis L., Norman J.A. 2008c. Habitat shifts in the evolutionary history of a Neotropical flycatcher lineage from forest and open landscapes. BMC Evol. Biol. 8:193.

Downloaded from http://sysbio.oxfordjournals.org/ at Ernst Mayr Library of the Museum Comp Zoology, Harvard University on February 24, 2014

Ridgely R.S., Greenfield P.J. 2001. The birds of Ecuador. Vol. 1. Ithaca (NY): Comstock Publishing Associates.
Ridgely R.S., Tudor G. 1994. The birds of South America. Vol. II. The suboscine passerines. Austin: University of Texas Press.
Schulenberg T.S., Stotz D.F., Lane D.F., O'Neill J.P., Parker T.A. 2007. Birds of Peru. Princeton (NJ): Princeton University Press.
Seehausen O. 2004. Hybridization and adaptive radiation. Trends Ecol. Evol. 19:198–207.
Slatkin M., Pollack J.L.L. 2008. Subdivision in an ancestral species creates asymmetry in gene trees. Mol. Biol. Evol. 25:2241–2246.
Stamos D.N. 2003. The species problem: biological species, ontology, and the metaphysics of biology. Lanham: Lexington Books.
Staubach F., Lorenc A., Messer P.W., Tang K., Petrov D.A., Tautz D. 2012. Genome patterns of selection and introgression of haplotypes in natural populations of the house mouse (*Mus musculus*). PLoS Genet. 8:e1002891.
Stoddard M.C., Prum R.O. 2008. Evolution of avian plumage color in a tetrahedral color space: a phylogenetic analysis of New World buntings. Am. Nat. 171:755–776.
Swofford D.L. 2003. PAUP*: phylogenetic analysis using parsimony (*and other methods). Version 4. Sunderland (MA): Sinauer Associates.
Traylor M.A. 1979. Check-list of birds of the world. Vol. VIII. Cambridge (MA): Museum of Comparative Zoology.
Uy J.A.C., Moyle R.G., Filardi C.E., Cheviron Z.A. 2009. Difference in plumage color used in species recognition between incipient species is linked to a single amino acid substitution in the melanocortin-1 receptor. Am. Nat. 174:244–254.
Vorobyev M., Osorio D. 1998. Receptor noise as a determinant of colour thresholds. Proc. R. Soc. Lond. Ser. B. 265:315–358.
Vorobyev M., Osorio D., Bennett A.T.D, Marshall N.J., Cuthill I.C. 1998. Tetrachromacy, oil droplets and bird plumage colors. J. Comp. Physiol. A. 183:621–633.
Walsh N., Dale J., McGraw K.J., Pointer M.A., Mundy N.I. 2012. Candidate genes for carotenoid colouration in vertebrates and their expression profiles in the carotenoid-containing plumage and bill of a wild bird. P. Roy. Soc. B 279:58–66.
Willing E.-M., Dreyer C., van Oosterhout C. 2012. Estimates of genetic differentiation measured by F_{ST} do not necessarily require large sample sizes when using many SNP markers. PLoS ONE 7: e42649.
Zerbino D.R., Birney E. 2008. Velvet: algorithms for de novo short read assembly using de Bruijn graphs. Genome Res. 18:821–829.
Zimmer J.T. 1941. Studies of Peruvian birds. Number XXXVII. Am. Mus. Novit. 1109:1–25.

Downloaded from http://sysbio.oxfordjournals.org/ at Ernst Mayr Library of the Museum Comp Zoology, Harvard University on February 24, 2014